

values. Since the calculations have been made assuming an equal energy for either cis or trans form, this result implies that the cis form is in practice more stabilized than the trans form in these solvents. In D<sub>2</sub>O solution the observed cis fraction showed a distinct minimum at  $n = 10$ . For longer chains the calculated chain length dependence agreed well with the observed ones in the three different solvents. The qualitative agreement was also observed for the fractions of dyad sequences in D<sub>2</sub>O solution (Figure 11) with the Monte Carlo results (Figure 9). As in the case of cis fraction, the calculated chain length dependences of the dyad sequences for longer chains agreed well with the observed ones. As compared with the Monte Carlo results, however, the observed cis,cis fraction was considerably larger and the trans,trans fraction was smaller. The anomalous behavior observed for shorter chains may be a result of specific end effects which depend strongly on the nature of the solvent.

## References and Notes

- (1) P. J. Flory, "Statistical Mechanics of Chain Molecules", Interscience, New York, N.Y., 1969.
- (2) K. K. Knaell and R. A. Scott III, *J. Chem. Phys.*, **54**, 566 (1971).
- (3) K. K. Knaell and R. A. Scott III, *J. Chem. Phys.*, **54**, 3556 (1971).
- (4) H. E. Warvari, K. K. Knaell, and R. A. Scott III, *J. Chem. Phys.*, **54**, 2020 (1971).
- (5) H. E. Warvari, K. K. Knaell, and R. A. Scott III, *J. Chem. Phys.*, **56**, 2903 (1972).
- (6) H. E. Warvari, K. K. Knaell, and R. A. Scott III, *J. Chem. Phys.*, **57**, 1146 (1972).
- (7) H. E. Warvari and R. A. Scott III, *J. Chem. Phys.*, **57**, 1154 (1972).
- (8) H. E. Warvari, K. K. Knaell, and R. A. Scott III, *J. Chem. Phys.*, **57**, 1161 (1972).
- (9) S. Tanaka and A. Nakajima, *Macromolecules*, **5**, 708 (1972).
- (10) S. Tanaka and A. Nakajima, *Macromolecules*, **5**, 714 (1972).
- (11) S. Premilat and J. Hermans, Jr., *J. Chem. Phys.*, **59**, 2602 (1973).
- (12) J. C. Howard, F. A. Momany, R. H. Andreatta, and H. A. Scheraga, *Macromolecules*, **6**, 535 (1973).
- (13) S. Tanaka and A. Nakajima, *Polym. J.*, **1**, 71 (1970).
- (14) F. A. Bovey, J. J. Ryan, and F. P. Hood, *Macromolecules*, **1**, 305 (1968).
- (15) M. Sisido, Y. Imanishi, and T. Higashimura, *Biopolymers*, **11**, 399 (1972).
- (16) S. Tanaka and A. Nakajima, *Polym. J.*, **2**, 717 (1971).
- (17) A. W. Burgess, Y. Paterson, and S. J. Leach, *J. Polym. Sci., Polym. Symp.*, **49**, 75 (1975).
- (18) C. H. Bamford, A. Elliott, and W. E. Hanby, "Synthetic Polypeptides", Academic Press, New York, N.Y., 1956, Chapter 3.
- (19) F. Conti and P. DeSantis, *Biopolymers*, **10**, 2581 (1971).
- (20) W. L. Mattice, *Macromolecules*, **6**, 855 (1973).
- (21) K. Titlestad, P. Groth, and J. Dale, *J. Chem. Soc., Chem. Commun.*, 646 (1973).
- (22) K. Titlestad, P. Groth, J. Dale, and M. Y. Ali, *J. Chem. Soc., Chem. Commun.*, 346 (1973).
- (23) F. T. Wall and J. J. Erpenbeck, *J. Chem. Phys.*, **30**, 634 (1959).
- (24) O. Kratky and G. Porod, *Recl. Trav. Chim. Pays-Bas*, **68**, 1106 (1949).
- (25) J. J. Hermans and R. Ullman, *Physica*, **18**, 951 (1952).
- (26) M. Sisido, Y. Imanishi, and T. Higashimura, *Macromolecules*, **9**, 320 (1976).
- (27) K. Nagai, *J. Chem. Phys.*, **38**, 924 (1963).
- (28) In the Nagai's series expansion (eq 10), the continuity of the end-to-end distance distribution is tacitly assumed. In real chains, however, the end-to-end distance cannot take values larger than that for maximum extension. The effect of this difference becomes more prominent when higher even moments are considered and this is also a likely reason for the divergence of the distribution function truncated at a higher even moment.

## Geometrical Criteria for Formation of Coiled-Coil Structures of Polypeptide Chains<sup>1</sup>

Ken Nishikawa and Harold A. Scheraga\*

Department of Chemistry, Cornell University, Ithaca, New York 14853.  
Received October 16, 1975

**ABSTRACT:** Crick's general formulas describing a coiled coil are expressed in a different form to combine the parameters of a coiled coil with the backbone dihedral angles of a polypeptide chain, assuming that the bond lengths and bond angles of the chain are fixed. While the existence of a low-energy coiled-coil conformation depends on energetic considerations, these formulas, which pertain to single-stranded structures and, by application of symmetry operations, to multistranded structures, provide the geometrical criteria for the existence of coiled coils. The concept of "the averaged structure of the minor helix", introduced here, makes it possible to relate the shape of the major helix to that of the minor helix. It is shown, in the analysis of a simple model of a single-stranded coiled-coil  $\beta$  structure, that strong geometrical restrictions exist for the formation of coiled-coil structures from a given minor helix conformation of a polypeptide chain; these restrictions are expressed in a general form that is applicable to any coiled-coil of any number of residues in a repeat unit. As an application, the possible existence of a two-stranded coiled-coil antiparallel  $\beta$  structure is considered, both geometrically and energetically, and discussed in relation to the observed twisted  $\beta$  structures in globular proteins. The proposed coiled-coil models of  $\alpha$ -helical proteins are also examined briefly.

It has been widely accepted that some of the fibrous proteins are in the form of coiled coils. For example, collagen exists as a three-stranded coiled coil,<sup>2,3</sup>  $\alpha$ -keratin probably as a three-stranded  $\alpha$ -helical coiled coil,<sup>4,5</sup> and muscle proteins<sup>6</sup> (especially tropomyosin<sup>7</sup>) as two-stranded  $\alpha$ -helical coiled coils. Each of these coiled-coil models has been deduced from x-ray diffraction data on fibers rather than on single crystals; however, the coiled-coil model for collagen has been supported by a recent crystal structure determination<sup>8</sup> of the repeating polytripeptide (Pro-Pro-Gly)<sub>10</sub>.

Crick has derived a general formula<sup>9</sup> which relates the parameters of the major and minor helices, the minor helix being the small one (e.g., the  $\alpha$  helix) and the major helix being the larger one which coils with a larger period than the smaller

one. Crick's formula pertains to a coiled-coil polypeptide chain in which the geometry (bond lengths and bond angles) varies continuously and periodically from one residue to another.<sup>10</sup> However, most treatments of polypeptide chains (including the computation of conformational energies) consider the geometry to be rigid and the peptide groups to be in the planar trans form, and use only the dihedral angles for rotation about single bonds as variables. Therefore, in the treatment developed in this paper, we will assume rigid geometry.

We do not deal here (except for a brief example in section III) with the intra- and intermolecular energetic criteria which determine whether a coiled coil exists and, if so, how many chains constitute the coiled-coil structure. However, this question is treated elsewhere<sup>11</sup> for the collagenlike repeating

tripeptide poly(Gly-Pro-Pro). Our concern here is only with the *geometrical* relations between the major and minor helices. A simple helix, e.g., the  $\alpha$  helix, can be twisted into a coiled-coil form by imposing a slight deformation on the successive backbone dihedral angles in the  $m$  ( $\geq 2$ ) repeating residues. The parameters of the major helix of the resulting coiled coil are not independent but are restricted to a certain range, depending on the helicity of the starting simple helix; by a "simple helix" here, we mean the "averaged structure of the minor helix", to be defined in section I. This problem has never been investigated systematically. Energy calculations would be required to select the most stable structure from among the geometrically allowed coiled coils.

Hopfinger and Walton<sup>12</sup> and Tumanyan<sup>13</sup> used rigid geometry in computing the conformational energies of coiled coils. However, Hopfinger and Walton varied the dihedral angles of two successive residues of the minor helix [of single-stranded poly(L-proline)], without showing the relation between the minor and major helices; i.e., they treated the coiled coil essentially as a simple helix in which the repeating unit was two residues instead of one. Tumanyan, likewise, varied the dihedral angles of three successive residues of the minor helix, in treating triple-stranded collagen. In these treatments,<sup>12,13</sup> the concept of the minor helix appears only implicitly in the fact that the repeating unit consists of two (and three) residues instead of one. In this paper, the coiled-coil parameters are combined with the backbone dihedral angles, and the relation between the major and minor helices of a single-stranded coiled coil is examined.

In section I, Crick's formula (eq 6 of ref 9), which was used to treat the Fourier transform of a coiled coil, will be cast in a different form to be combined, in a general way, with the backbone dihedral angles, following the method of Sugeta and Miyazawa<sup>14</sup> which was developed for the treatment of simple helices.

In section, II, we concentrate on a particular case, that of the coiled-coil form of the  $\beta$  structure. In a two-stranded  $\beta$  structure (either parallel or antiparallel), there are two hydrogen bonds in every second residue. Therefore, the repeating unit of such a  $\beta$  structure consists of two residues, and the pairs of hydrogen bonds are equivalent from one repeating unit to another. We will find that the parameters of the coiled-coil major helix depend on the averaged structure of the minor helix, and that the approximate relation between these is applicable to any coiled-coil system, in general. Using these approximate relations, which hold only for the case of small chain deformations, the coiled-coil major helix of a given averaged structure of the minor helix can be described by two independent parameters, no matter how many residues are in the repeating unit.

As an application of the method developed here, we will combine it with energy calculations, in section III, to examine the possible existence of coiled-coil forms of two-stranded antiparallel  $\beta$  structures. In section IV, we will discuss the results of section III in connection with the observed<sup>15</sup> right-handed twist of the  $\beta$  structures in globular proteins. In section V, we will examine briefly the coiled-coil models proposed for the  $\alpha$  proteins in light of the general features of coiled coils that are brought out in the present study.

### I. Relation between Coiled-Coil Parameters and Dihedral Angles of the Constituent Polypeptide Chain

Consider a polypeptide coiled coil with  $m$  amino acid residues in the repeating unit (where  $m$  is an integer  $\geq 2$ ;  $m = 1$  describes a simple helix). Let a reference atom A (e.g., the  $C^\alpha$  atom of the first residue of the repeating unit) in the  $j$ th repeating unit be designated as  $A_{jm}$  (see Figure 1 for the positions of  $A_0$ ,  $A_m$  and  $A_{2m}$ ). Following Crick,<sup>9</sup> the positions of

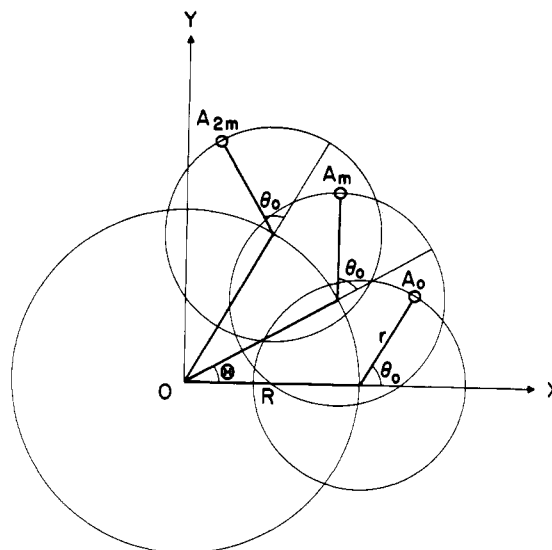


**Figure 1.** Schematic representation of a single-stranded coiled coil with  $m$  amino acid residues in the repeating unit, the positive  $z$  axis coming up, perpendicular, from the plane of the paper. The large circle is the cross section of the major helix of radius  $R$ , and rotation (per  $m$  residues)  $\Theta$ . The small circles are the cross sections of the minor helix of radius  $r$ , showing the positions of the reference atoms  $A_0$ ,  $A_m$ , and  $A_{2m}$  at an orientation angle  $\theta_0$  with respect to the radial direction ( $x'$  axis);  $\theta_0$  is measured in the  $x'$ ,  $y'$ ,  $z'$  coordinate system, and atom  $A_{jm}$  is in the  $x'$ - $y'$  plane.

$A_{jm}$  are given in a rotating coordinate system,  $x'$ ,  $y'$ ,  $z'$ , by

$$\begin{aligned} x' &= r \cos(jm\theta + \theta_0) \\ y' &= r \sin(jm\theta + \theta_0) \\ z' &= 0 \end{aligned} \quad (1)$$

where  $r$  is the radius of the minor helix (with respect to the reference atom A),  $\theta$  is the angular repeat per residue (measured in the rotating frame), and  $\theta_0$  is the orientation of atom  $A_{jm}$  with respect to the  $x'$  axis in the  $x'$ ,  $y'$ ,  $z'$  coordinate system (see Figure 1). The origin of the  $x'$ ,  $y'$ ,  $z'$  system traces out the major helix, and the coordinates of this origin in the fixed coordinate system,  $x$ ,  $y$ ,  $z$ , of the major helix are given by

$$\begin{aligned} x &= R \cos(j\Theta) \\ y &= R \sin(j\Theta) \\ z &= jH \end{aligned} \quad (2)$$

where  $R$  is the radius of the major helix,  $\Theta$  is the rotation around the  $z$  axis per  $m$  residues, and  $H$  is the advance along the  $z$  axis per  $m$  residues. The  $x'$ ,  $y'$ ,  $z'$  system has its  $z'$  axis tangential to the major helix (at an angle  $\alpha$  with respect to the  $z$  axis) and its  $x'$  axis radial and perpendicular to the  $z$  axis. Thus, as  $\Theta$  varies, the  $x'$ ,  $y'$ ,  $z'$  axes follow the major helix, with the  $x'$  axis always pointing directly away from the  $z$  axis. Since  $A_{jm}$  is always in the  $x'y'$  plane,  $z' = 0$ . The angle  $\alpha$ , which is called the "pitch angle",<sup>9</sup> is related to the parameters of the major helix by

$$\tan \alpha = \Theta R / H \quad (3)$$

The parameters  $R$ ,  $H$ , and  $r$  are defined to be always positive, and  $\theta$  and  $\theta_0$  can be positive or negative depending on whether the major and minor helices are right or left handed, respectively. Hence, according to eq 3, the sign of  $\alpha$  is always that of  $\Theta$ .

The correspondence between the parameters introduced

here and those used by Crick<sup>9</sup> is as follows (with Crick's parameters being on the right-hand side of these equations):

$$\begin{aligned} R &= r_0 \\ r &= r_1 \\ \Theta/m &= 2\pi N_0/M \\ \theta &= 2\pi N_1/M \\ (2\pi/\Theta)H &= P \end{aligned} \quad (4)$$

Crick's paper<sup>9</sup> should be consulted for the definitions of his parameters.

A coiled coil is a kind of simple helix with  $m$  residues in the repeating unit; i.e., the reference atom ( $A_0, A_m, A_{2m}$ , etc.) in every  $m$  residues forms a simple helix of rotation per  $m$  residues of  $\Theta$  and rise per  $m$  residues of  $H$ . However, the distance of  $A_{jm}$  from the  $z$  axis is not equal to  $R$ . Rather, the repeating reference atoms  $A_{jm}$  lie at a common orientation angle  $\theta_0$  with respect to the radial direction  $R$  (see Figure 1). In order for  $A_{jm}$  to preserve this common orientation angle (i.e., for the atoms  $A_{jm}$  to form a simple helix with an angular repeat per residue of  $\Theta$  in the stationary frame), the minor helix must make a complete turn in  $m$  residues, i.e.,

$$m\theta = 2n\pi \quad (5)$$

where  $n$  is an integer. Thus, the term  $jm\theta$  in eq 1, which is a multiple of  $2\pi$ , can be omitted. To transform the coordinates of atoms  $A_{jm}$  from the  $x', y', z'$  system (eq 1) to the  $x, y, z$  system, we rotate the  $x', y', z'$  system by  $-j\theta$  around the  $z$  axis, and by  $\alpha$  (of eq 3) around the  $x$  axis, and translate its origin from that given by eq 2 to the origin of the  $x, y, z$  system, and obtain

$$\begin{aligned} x &= R \cos(j\theta) + r \cos(j\theta) \cos \theta_0 - r \cos \alpha \sin(j\theta) \sin \theta_0 \\ y &= R \sin(j\theta) + r \sin(j\theta) \cos \theta_0 + r \cos \alpha \cos(j\theta) \sin \theta_0 \\ z &= jH - r \sin \alpha \sin \theta_0 \end{aligned} \quad (6)$$

which is the same as the first equation on p 687 of ref 9.

It can be seen from eq 6 that five parameters are required to specify a coiled-coil structure (for a given value of  $m$ ); three of these are  $\Theta, H$ , and  $R$  for the major helix, and the other two parameters,  $r$  and  $\theta_0$ , specify the positions of the reference atoms  $A_{jm}$  with respect to the (curved) axis of the minor helix. Of these, the orientation parameter  $\theta_0$ , which is defined in the rotating frame, does not exist for a simple helix because there is no meaning to the relative orientations of the  $x', y', z'$  and  $x, y, z$  coordinate systems for a simple helix; thus,  $\theta_0$  is one of the parameters characterizing the coiled coil. The existence of this quantity implies that there is an extra degree of freedom in a coiled coil; i.e., even if the major helix is fixed in a given shape, characterized by the values of  $\Theta, H$ , and  $R$ , the minor helix can still be rotated about its own (curved) axis.

The parameter  $\theta$ , eliminated from eq 1 by use of eq 5, has a different meaning from the usual rotation per residue of the minor helix;  $\theta$  is measured on a rotating frame, as described above, whereas the rotation per residue in a simple helix is defined by a stationary frame.

It should be noted that the number of residues,  $m$ , in the repeating unit is not a variable for a given coiled coil. It depends on the amino acid sequence or on interchain interactions in a given system. For example,  $m$  is 3 for collagen because of the characteristic appearance of glycine at every third residue in the amino acid sequence.<sup>16</sup> It is also determined by specific interactions between chains; e.g., Crick<sup>4</sup> treated side chains as knobs, and deduced a value of  $m = 7$  for  $\alpha$ -keratin, based on the "knob-hole" interactions between the side chains of different strands (a possible value for  $m$  for the  $\alpha$ -helical

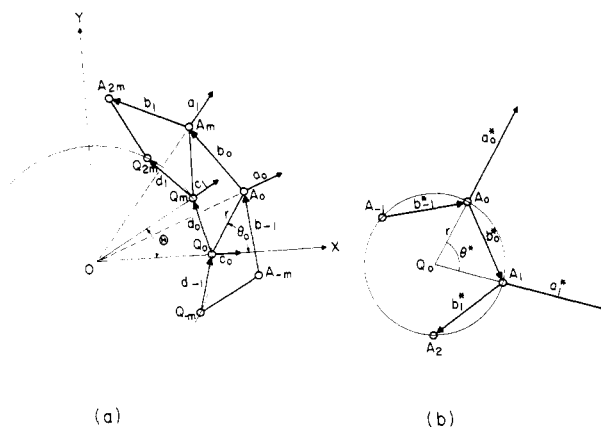


**Figure 2.** Schematic representation of (a) a single-stranded coiled coil (the same one of Figure 1), and (b) the corresponding averaged structure of the minor helix. In both (a) and (b) the helix is coming up out of the paper as  $i$  and  $j$  increase, and the sense of the major and minor helices shown in (a) and (b) are right handed and left handed, respectively. The points  $Q_{jm}$  and the various vectors are defined in the text. In (b)  $A_0$  and  $Q_0$  are in the plane of the paper, and  $A_1, A_2$ , etc., are above it. Atoms  $A_i$  (for  $i \neq jm$ ), of Figure 2b, which have different orientation angles ( $\theta_0$ ), are not shown in Figures 2a or 1 for simplicity.

coiled coil will be discussed from a different point of view in section V). Thus, we may regard the value of  $m$  as given by a priori considerations, i.e., by the characteristic nature of the system that participates in formation of a coiled-coil structure.

We now proceed to derive a relation between the backbone dihedral angles and the parameters of a single-stranded coiled coil. It is necessary to treat only the backbone conformation of the chain and, in this section, we will assume that the peptide group is in the planar trans conformation; variation of the dihedral angle<sup>17</sup>  $\omega$  will be taken into consideration in section II. Then, a coiled-coil structure of a polypeptide chain is given by the set of dihedral angles<sup>17</sup> of the  $m$  residues in the repeating unit,  $\phi_1, \psi_1, \phi_2, \psi_2, \dots, \phi_m, \psi_m$ . Since each value of  $\phi_i, \psi_i$  will differ slightly from one residue to another in a coiled-coil structure, we denote them by

$$\begin{aligned} \phi_i &= \phi^* + \Delta\phi_i \quad (i = 1, 2, \dots, m) \\ \psi_i &= \psi^* + \Delta\psi_i \quad (i = 1, 2, \dots, m) \end{aligned} \quad (7)$$

where  $\phi^*$  and  $\psi^*$  are the averaged values of  $\phi_i$  and  $\psi_i$ , respectively, over the  $m$  residues in the repeating unit, i.e.,

$$\begin{aligned} \sum_{i=1}^m \Delta\phi_i &= 0 \\ \sum_{i=1}^m \Delta\psi_i &= 0 \end{aligned} \quad (8)$$

The quantities  $\phi^*$  and  $\psi^*$  define a simple straight helix, which we call the "averaged structure of the minor helix". The deformation from the averaged structure, given by  $\Delta\phi_i$  and  $\Delta\psi_i$ , makes its helix axis twist to give a coiled-coil structure. The helical parameters for the averaged minor helix may be defined in the usual way:  $\theta^*$  is the rotation per residue and  $h^*$  is the rise per residue.

In order to relate the dihedral angles to the coiled-coil parameters presented in eq 6, the axis of the minor helix is specified in terms of the dihedral angles. While this is difficult to do, in general, because the axis of the minor helix is not straight, it can be accomplished with the aid of the averaged structure of the minor helix. The origin of the rotating coordinate system of eq 1, denoted as  $Q_{jm}$ , is defined as the center of the cross-section of the averaged minor helix at reference atom  $A_{jm}$  (Figure 2b). The points,  $Q_{jm}$ , trace the major helix

given by eq 2 to make a simple helix of parameters  $\Theta$ ,  $H$ ,  $R$  (Figure 2a).

The radius of the minor helix is defined simply as the radius of the averaged minor helix, so that the radius  $r$  for atom  $A_i$ , and the vector  $\mathbf{r}$  ( $= \overrightarrow{Q_0 A_i}$ ), are expressed in terms of the vector  $\mathbf{a}^*$  of the averaged minor helix (Figure 2b) by direct application of the Sugeta-Miyazawa procedure,<sup>14</sup> i.e., by

$$r = \frac{(a^*)^3}{2[(a^*)^2 - (\mathbf{a}^*_0 \cdot \mathbf{a}^*_1)]} \quad (9)$$

and

$$\mathbf{r} = (r/a^*)\mathbf{a}^*_0 \quad (10)$$

where  $a^*$  is the length of the vector  $\mathbf{a}^*$ . The vectors  $\mathbf{a}^*_i$  ( $i = 0, 1, 2, \dots$ ) are functions of the dihedral angles,<sup>14</sup> i.e., of  $\phi^*$  and  $\psi^*$ ; thus, the radius  $r$  depends only on  $\phi^*$  and  $\psi^*$  of eq 7.

The other coiled-coil parameters are related to the dihedral angles ( $\phi_i, \psi_i$ ), by essentially the same procedure as that developed by Sugeta and Miyazawa<sup>14</sup> for a simple helix. However, two kinds of reference "atoms",  $A_{jm}$  and  $Q_{jm}$ , instead of one, are required for a coiled coil. All of the vectors  $\mathbf{a}_i$ ,  $\mathbf{b}_i$ ,  $\mathbf{c}_i$ , and  $\mathbf{d}_i$  ( $i = 0, \pm 1, \pm 2, \dots$ ) shown in Figure 2a, and their lengths, are functions of the dihedral angles  $\phi_i, \psi_i$  (see Appendix A for the details). With  $r$  being given by eq 9, the remaining coiled-coil parameters  $\Theta$ ,  $H$ ,  $R$ , and  $\theta_0$  can be expressed in terms of these vectors, as follows:

$$\cos \Theta = (\mathbf{a}_0 \cdot \mathbf{a}_1)/a^2 \quad (11)$$

$$H \sin \Theta = \mathbf{b}_0 \cdot (\mathbf{a}_0 \times \mathbf{a}_1)/a^2 \quad (12)$$

$$R(1 - \cos \Theta) = c/2 \quad (13)$$

$$\cos \theta_0 = (\mathbf{r} \cdot \mathbf{c}_0)/rc \quad (14)$$

$$\sin \theta_0 = \pm(1 - \cos^2 \theta_0)^{1/2} \quad (15)$$

where the sign in eq 15 should correspond to that of the product  $\mathbf{d}_0 \cdot (\mathbf{c}_0 \times \mathbf{r})$ . Thus, all of the parameters in eq 6 have been expressed as functions of the backbone dihedral angles.

Crick<sup>9</sup> and Fraser et al.<sup>10</sup> generated coiled-coil structures by use of eq 6, i.e., by placing each atom of the polypeptide in accordance with eq 6. However, we note that this "ideal" type of coiled coil cannot have (fixed) rigid geometry; i.e., the geometry of the constituent peptide chain varies from one residue to another.<sup>10</sup> For example, the  $C^{\alpha}_i \cdots C^{\alpha}_{i+1}$  distance is not a constant quantity under such conditions. The reason for this is that the curvature of the minor helix differs between its inside and outside surface, because the axis of the minor helix is not straight. On the other hand, we will maintain (fixed) rigid geometry in this paper, and generate a coiled coil, not from eq 6, but from the backbone dihedral angles in the repeating unit; the coiled-coil parameters will be calculated from eq 9 and 11–15.

The difference between the above two methods for generating a coiled coil lies in the meaning of the orientation angle  $\theta_0$  of eq 6. Following Crick,<sup>9</sup> all atoms of the same kind (say, the  $C^{\alpha}$  atoms) in a coiled coil of, say, two residues per repeating unit have the successively alternating angles of  $\theta_0$  and  $180^\circ + \theta_0$  (but with  $\theta_0$  being different for each kind of atom). In our procedure, a given kind of atom will have the same value of  $\theta_0$  in every  $m$  residues. However, the orientation angle of atom  $A_i$  (for  $i \neq jm$ ) will not take on the exact value given above (say,  $180^\circ + \theta_0$  for  $m = 2$ ), but will deviate slightly from this "ideal" position. The precise value of  $\theta_0$  for any atom is determined subsequently by the given values of the dihedral angles (by eq 14 and 15).

Multistranded coiled coils, which will be considered later (in section III), are constructed by applying a symmetry operation to a single-stranded coiled coil, as described by Parry and Suzuki<sup>18</sup> (see also ref 11).

## II. Relation between the Major Helix and the Averaged Structure of the Minor Helix

From eq 7, we see that a coiled coil can be thought of as being constructed by slight variations ( $\Delta\phi_i$  and  $\Delta\psi_i$ ) from a simple helical conformation ( $\phi^*$  and  $\psi^*$ ). The minor helix is specified by  $\phi^*$  and  $\psi^*$  (and, at the same time, the radius  $r$  is determined by eq 9), and the shape of the major helix ( $\Theta$ ,  $H$ , and  $R$ ) and the orientation of the minor helix ( $\theta_0$ ) are determined by  $\Delta\phi_i$  and  $\Delta\psi_i$ ; thus, the coiled coil is completely specified in terms of  $\phi_i$  and  $\psi_i$ . The question then arises as to whether and how the shape of the major helix is restricted when the averaged structure of the minor helix is fixed. Therefore, in this section we will develop the relation between  $\Theta$ ,  $H$ , and  $R$  of the major helix and  $\theta^*$  and  $h^*$  (or  $\phi^*$  and  $\psi^*$ ) of the averaged structure of the minor helix. For this purpose, we select various sets of  $\phi^*$  and  $\psi^*$ , and compute  $\phi_i$  and  $\psi_i$  for various values of  $\Delta\phi_i$  and  $\Delta\psi_i$  for each set of  $\phi^*$  and  $\psi^*$  (see eq 7); then  $\Theta$ ,  $H$ , and  $R$  are computed from eq 11–13.

As an illustrative model for this calculation, we have chosen the extended (or  $\beta$ ) structure. For this model,  $m = 2$  since there are two hydrogen bonds in every second residue, and the pairs of hydrogen bonds are taken to be equivalent from one two-residue repeating unit to another; i.e., the same orientation angle  $\theta_0$  (Figure 1) occurs at every second residue. While the  $\beta$ -pleated sheet structure is an assembly (in parallel or antiparallel fashion), in this section we are considering only a single strand, and will use the above description of the interchain hydrogen bonding (which applies to both parallel and antiparallel chains) to define the value of  $m$ . The bond lengths and bond angles are taken as those of an L-alanine residue.<sup>19</sup> Two possibilities will be considered for the dihedral angle  $\omega$ , one in which it is fixed at  $180^\circ$  (planar trans position), and one in which  $\omega$  is allowed to vary (around the position  $\omega = 180^\circ$ ). For this model, the dihedral angles in a repeating unit may be expressed as

$$\begin{aligned} \phi_1 &= \phi^* + \Delta\phi & \phi_2 &= \phi^* - \Delta\phi \\ \psi_1 &= \psi^* + \Delta\psi & \psi_2 &= \psi^* - \Delta\psi \\ \omega_1 &= \pi + \Delta\omega & \omega_2 &= \pi - \Delta\omega \end{aligned} \quad (16)$$

where  $\Delta\omega$  will be taken as zero or as a variable for the two different sets of calculations. Since  $\phi^*$  and  $\psi^*$  are fixed, there are only three variables (including  $\Delta\omega$ ) in this model. It might seem strange to compute four parameters ( $\Theta$ ,  $H$ ,  $R$ , and  $\theta_0$ , since  $r$  is now constant) from three variables, but this apparent difficulty will be disposed of in the last paragraph of this section.

The choice of  $\phi^*$  and  $\psi^*$  is arbitrary, for the present illustrative purpose of generating coiled coils. Ten different points in the antiparallel  $\beta$ -structure region of a  $\phi, \psi$  map (Figure 3) were chosen. Five of these ( $B_L, C_L, D_L, E_L, F_L$ ) were arbitrarily chosen to lie on the line  $\psi^* = 140^\circ$ , and have the values of  $\theta^*$  shown in Figure 3; since  $\theta^* < 0$ , these are left-handed minor helices. The right-handed minor helical structures ( $B_R, C_R, D_R, E_R, F_R$ ) were chosen to have the same values of  $h^*$  (with  $\theta^*$  having the same, but positive, values) as the corresponding left-handed structures (see Table I). The quantity  $\Theta_0$  listed in Table I is the angular repeat per two residues in each averaged minor helix, i.e.,

$$\Theta_0 \equiv m\theta^* - 2n\pi \quad (17)$$

Here the integer  $n$  is chosen uniquely so that the value of  $\Theta_0$  falls in the range of  $-180$  to  $180^\circ$  for the given values of  $\theta^*$  and  $m$  ( $=2$ ). The approximation,  $\Theta \sim \Theta_0$ , which holds when the pitch angle  $\alpha$  is small, has been used by various authors<sup>2-4</sup> to estimate the value of  $\Theta$  for a given minor helix. From the values of  $\Theta_0$  given in Table I, we may expect that coiled coils

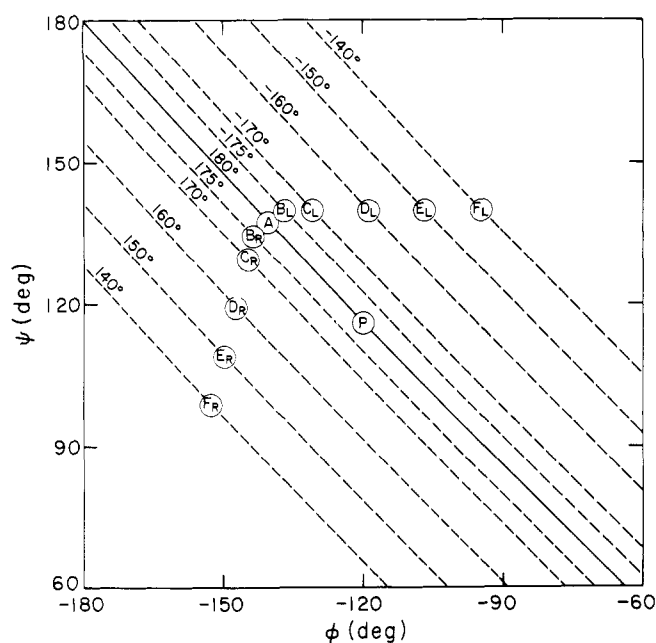


**Figure 3.** Extended structure region of a  $\phi, \psi$  map. The dashed lines are contours of constant  $\theta^*$ , the angular repeat per residue in the averaged structure of the minor helix in a coiled-coil  $\beta$  structure. The solid line is the contour for  $\theta^* = 180^\circ$ , i.e., for the structure with twofold screw symmetry. The typical<sup>22</sup> antiparallel (A) and parallel (P) structures lie on the  $\theta^* = 180^\circ$  contour. The circles (except for P) indicate the conformations chosen to specify the sets of values of  $\phi^*$  and  $\psi^*$ .

**Table I**  
Representative Conformations of the Averaged Minor Helix for the Coiled-Coil  $\beta$  Structure

	$\Theta_0, ^\circ$ deg	$\phi^*, \text{deg}$	$\psi^*, \text{deg}$	$\theta^*, \text{deg}$	$h^*, \text{\AA}$
A <sup>b</sup>	0	-140.4	137.6	180	3.445 <sup>c</sup>
B <sub>L</sub>	10	-136.7	140.0	-175	3.443
C <sub>L</sub>	20	-130.7	140.0	-170	3.420
D <sub>L</sub>	40	-118.7	140.0	-160	3.366
E <sub>L</sub>	60	-106.7	140.0	-150	3.297
F <sub>L</sub>	80	-94.5	140.0	-140	3.211
B <sub>R</sub>	-10	-143.8	134.9	175	3.443
C <sub>R</sub>	-20	-144.8	129.6	170	3.420
D <sub>R</sub>	-40	-147.3	119.5	160	3.366
E <sub>R</sub>	-60	-149.8	109.3	150	3.297
F <sub>R</sub>	-80	-152.5	99.1	140	3.211

<sup>a</sup> From eq 17. <sup>b</sup> The typical antiparallel  $\beta$  structure, listed here as a reference. <sup>c</sup> Taken from ref 20.

constructed from conformations B<sub>L</sub>, C<sub>L</sub>, etc., will be right handed, with the approximate values of  $\Theta_0$  listed; likewise, the coiled coils from B<sub>R</sub>, C<sub>R</sub>, etc., will be left handed.

For each set of values of  $\phi^*, \psi^*$  of Table I,  $\Theta, H, R$ , and  $\theta_0$  are computed by use of eq 11-15. When  $\omega$  was held fixed (i.e.,  $\Delta\omega = 0^\circ$ ),  $\Delta\phi$  and  $\Delta\psi$  were varied from  $-20$  to  $20^\circ$  in  $2^\circ$  intervals. When  $\omega$  was not held fixed (i.e.,  $\Delta\omega \neq 0^\circ$ ),  $\Delta\phi$  and  $\Delta\psi$  were varied from  $-20$  to  $20^\circ$ , and  $\Delta\omega$  from  $-10$  to  $10^\circ$ , all three in  $4^\circ$  intervals.

The computations lead to a distribution of values of ( $\Theta, H, R, \theta_0$ ) at each grid point of  $\Delta\phi, \Delta\psi$  (and  $\Delta\omega$ ) in the ranges chosen above, for each averaged minor helix listed in Table I. The results may be shown by plotting the calculated values of  $\Theta$  (and, separately,  $H$  and  $R$ ) against  $\alpha$  which is also calculated at each grid point from eq 3. Figures 4-6 show plots of

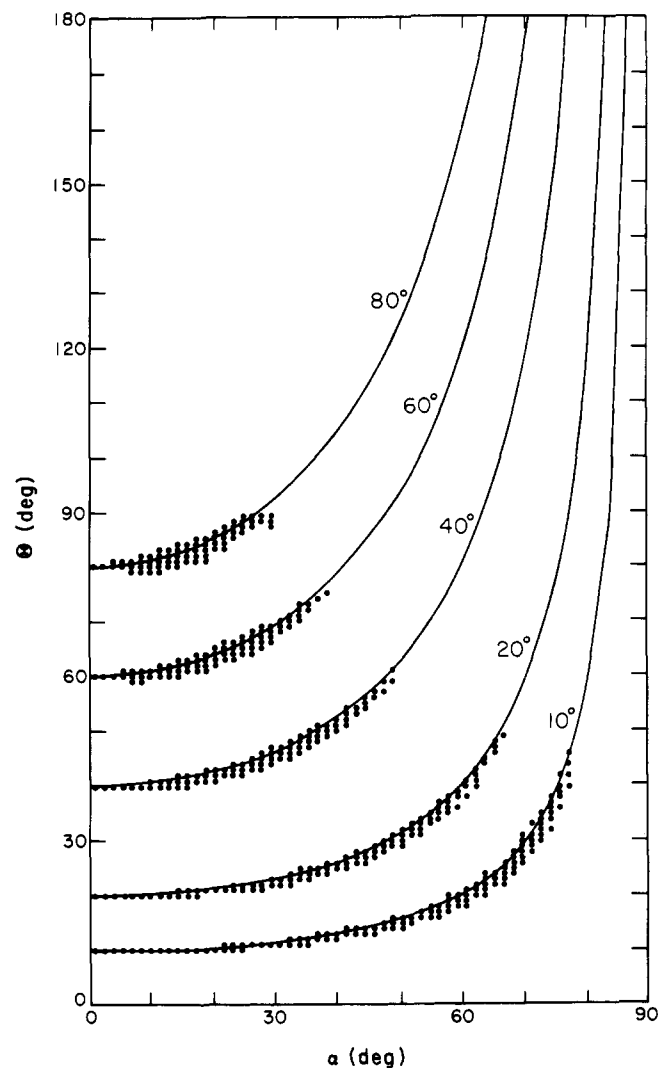


**Figure 4.** Plots of  $\Theta$  vs.  $\alpha$  for the values of  $\Theta_0$  listed on each curve. The dots are the calculated values, and the solid lines are the theoretical approximations (eq 22) for the different values of  $\Theta_0$  listed in Table I. Each dot for a particular value of  $\Theta_0$  corresponds to a different grid point in the  $\Delta\phi, \Delta\psi$  space (for  $\Delta\omega = 0^\circ$ ). The total number of calculated points was the same for each value of  $\Theta_0$ ; however, the representation by dots is schematic because of the overlap of dots that would occur if they were all plotted exactly.

$\Theta$  vs.  $\alpha$ ,  $H$  vs.  $\alpha$ , and  $R$  vs.  $\alpha$ , respectively, for  $\Delta\omega = 0^\circ$ , for the left-handed minor helices B<sub>L</sub>, C<sub>L</sub>, etc. (indicated by the value of  $\Theta_0$ ). Each dot in the plots corresponds to a different value of ( $\Delta\phi, \Delta\psi$ ). It can be seen clearly that, for a given structure of the minor helix, the distribution of major helices (for different values of  $\Delta\phi$  and  $\Delta\psi$ ) is discrete and very narrow in all cases, i.e., the dots for the various values of  $\Theta_0$  do not overlap. Interestingly, the right-handed minor helices B<sub>R</sub>, C<sub>R</sub>, etc. (not shown here) give the same distributions of Figures 4-6, except that the signs of  $\Theta$  and  $\alpha$  are negative. This is not a trivial result, since the backbone conformations of B<sub>L</sub> and B<sub>R</sub>, for example, are not symmetrical with respect to a mirror plane (the mirror image of B<sub>L</sub> would have  $\phi^* = 136.7^\circ$  and  $\psi^* = -140.0^\circ$ , whereas B<sub>R</sub> has  $\phi^* = -143.8^\circ$  and  $\psi^* = 134.9^\circ$ ). Thus, the distribution of  $\Theta, H$ , and  $R$ , i.e., the shape of the major helix, appears to be limited essentially by the parameters  $\theta^*$  and  $h^*$  of the averaged minor helix rather than by the geometry and dihedral angles of the chain; i.e., various sets of bond lengths, bond angles, and dihedral angles could lead to the same values of  $\theta^*$  and  $h^*$ , and it is  $\theta^*$  and  $h^*$  which restrict the values of  $\Theta, H$ , and  $R$ .

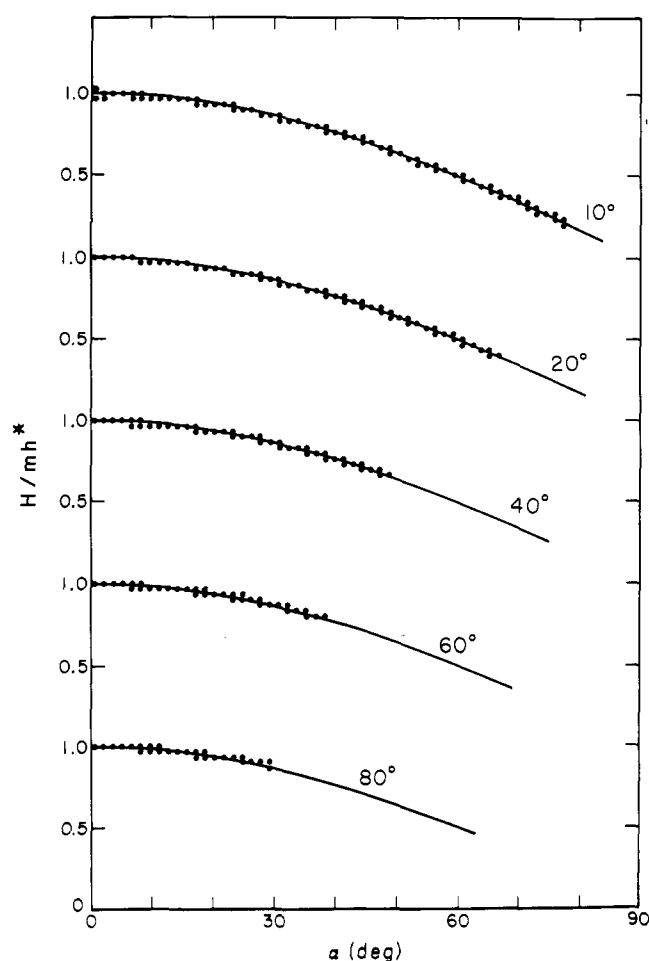


**Figure 5.** Plots of  $H$  vs.  $\alpha$  for the values of  $\theta_0$  listed on each curve. The dots are the calculated values, and the solid lines are the theoretical approximations (eq 20) for the different values of  $\theta_0$  listed in Table I. See the legend of Figure 4 for further remarks. It should be noted that the ordinate is normalized as  $H/mh^*$  (with  $m = 2$  in this example), and the frame is shifted upwards for each value of  $\theta_0$ .

This conclusion, that the distribution of  $\theta$ ,  $H$ , and  $R$  depends only on  $\theta^*$  and  $h^*$ , was tested by inclusion of  $\Delta\omega$  as an additional variable in the range of values described above. The resulting distributions (not shown here) were the same on the  $H$  vs.  $\alpha$  plot, but more spread out on the  $\theta$  vs.  $\alpha$  and  $R$  vs.  $\alpha$  plots. The wider spread in the distributions can be explained by the larger deformations of the polypeptide chain, where the chain deformation,  $\delta$ , may be taken as

$$\delta = [(\Delta\phi)^2 + (\Delta\psi)^2 + (\Delta\omega)^2]^{1/2} \quad (18)$$

The values of  $\delta$  are now larger because of the inclusion of  $\Delta\omega$ , since the ranges of  $\Delta\phi$  and  $\Delta\psi$  have not been changed. However, if the  $\Delta\phi$ ,  $\Delta\psi$  space is limited to less than the  $\pm 20^\circ$  used previously so that, with the inclusion of  $\Delta\omega \neq 0$ , the value of  $\delta$  is limited to a maximum of  $\pm 20^\circ$ , then essentially the same distributions as in Figures 4–6 are obtained. Thus, we may conclude that the shape of the major helix is limited by the helicity (i.e.,  $\theta^*$  and  $h^*$ ) of the minor helix, and that the chain deformation,  $\delta$ , determines the spread of the distribution.

As implied by these data, we may express the restriction of the major helix by its minor helix in the form of approximate, rather than rigorous (because of the distribution of dots on the curves of Figures 4–6), relations between  $(\theta, H, R)$  and  $(\theta^*, h^*)$ ; i.e., we may obtain approximate relations for the solid lines of Figures 4–6.

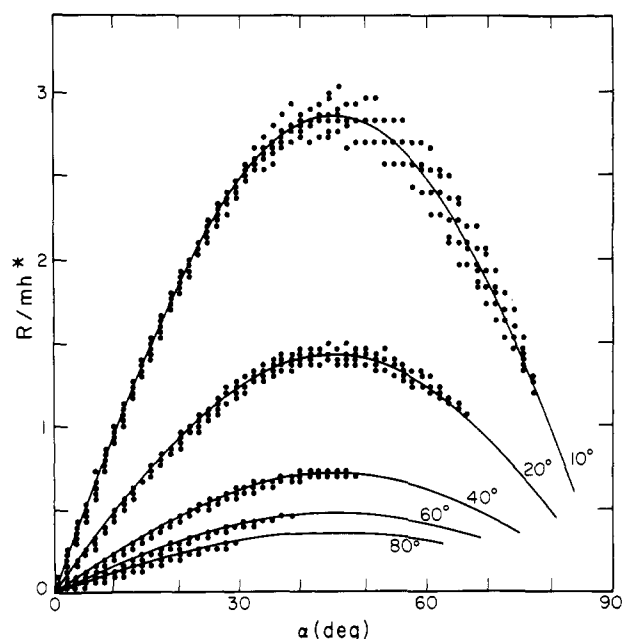


**Figure 6.** Plots of  $R$  vs.  $\alpha$  for the values of  $\theta_0$  listed on each curve. The dots are the calculated values, and the solid lines are the theoretical approximations (eq 23) for the different values of  $\theta_0$  listed in Table I. See the legend of Figure 4 for further remarks. It should be noted that the ordinate is normalized as  $R/mh^*$  (with  $m = 2$  in this example).

First, the  $H$  vs.  $\alpha$  data of Figure 5 are found empirically to fit the relation:

$$(H^2 + \theta^2 R^2)^{1/2} \simeq mh^* \quad (19)$$

The left-hand side of eq 19 is the distance from  $Q_0$  to  $Q_m$  measured along the major helical path (Figure 2), as can be seen by a flat representation (radial projection) of the major helix. The right-hand side of eq 19 is the distance from  $Q_0$  to  $Q_m$  of the averaged (straight) minor helix, i.e., the advance along the helix axis of the averaged minor helix. Thus, eq 19 says that these two distances are approximately equal. Substituting eq 3 into eq 19, we obtain

$$H \simeq (mh^*) \cos \alpha \quad (20)$$

The solid lines in Figure 5 are plots of  $H/mh^*$  (for  $m = 2$ ) vs.  $\alpha$ , according to eq 20. It should be noted that the parameter  $\theta^*$  is not included in eq 19 or eq 20. This explains why the  $H$  vs.  $\alpha$  plots for various values of  $\theta_0$  superimpose on each other (this is not obvious from Figure 5 because the curves were frame shifted for clarity).

In a similar way, approximate empirical relations may be obtained from the  $\theta$  vs.  $\alpha$  and  $R$  vs.  $\alpha$  data of Figures 4 and 6, viz.,

$$H\theta \simeq (mh^*)\theta_0 \quad (21)$$

The meaning of this relation can be understood with the aid of the flat representations (radial projections) of the helical structures shown in Figure 7. The "surface area" of the repeating unit of the averaged minor helix is seen to be  $(mh^*)\theta_0 r$ , and is almost equal to that of the minor helix ( $H\theta r$ ) of the coiled-coil structure. Substituting  $H$  of eq 20 into eq 21, we obtain

$$\theta \simeq \theta_0 / \cos \alpha \quad (22)$$

Equation 22 is an improved form of the rough approximation,  $\theta \sim \theta_0$ , and was used to obtain the solid lines of Figure 4. Then, the  $R$  vs.  $\alpha$  relation is derived by substituting eq 20 and 22 into eq 19, i.e.,

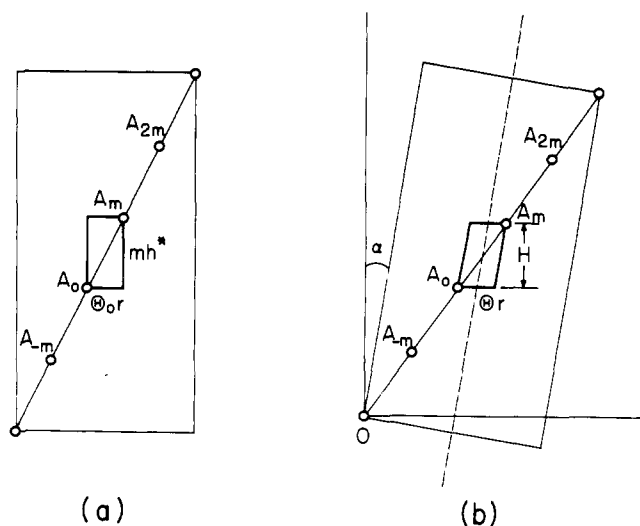


**Figure 7.** Flat representations (radial projections) of helices, obtained by cutting the cylindrical surface of the helix at a given value of  $r$  and opening it out flat. (a) The averaged structure of the minor helix; (b) the minor helix in a coiled-coil structure. The surface of the repeating unit is indicated by heavy lines in (a) and (b). The axis of the minor helix, indicated by a dashed line in (b), tilts at an angle  $\alpha$  from the vertical (the  $Oz$  direction of Figure 1). Actually, the lines in (b) should be curved because of the coiled coiling; i.e., the surface of the minor helix in a coiled coil cannot be opened out perfectly flat.

$$R \simeq (mh^*/\theta_0) \sin \alpha \cos \alpha \quad (23)$$

which is shown as solid lines, for different values of  $\theta_0$ , in Figure 6. It can be seen that all of the approximations hold well (i.e., pass through the centers of the distributions of dots, which depend on the magnitude of  $\delta$ ) in the wide range of  $\alpha$ , although the calculated values spread out at large values of  $\alpha$  on the  $\theta$  vs.  $\alpha$  and  $R$  vs.  $\alpha$  plots, as already mentioned.

Thus, we may regard eq 20, 22, and 23, or the equivalent eq 19 and 21 (with the elimination of  $\alpha$  by means of eq 3), as the approximate conditions relating the parameters of the major and minor helices. Several features of the coiled coil may then be deduced from these relations.

1. The sign of  $\theta$  is always the same as that of  $\theta_0$  (eq 22, with  $\alpha$  in the range of 0 to  $\pm 90^\circ$ ). In other words, the handedness of the major helix is completely determined by the sign of  $\theta_0$ , which in turn depends on  $\theta^*$  and  $m$  (see eq 17). For a positive value of  $\theta_0$  (right-handed major helix, thereby making  $\alpha$  positive), the approximate minimum value of  $\theta$  (intercept at  $\alpha = 0$  in Figure 4) is  $\theta_0$ . The situation is reversed for a negative value of  $\theta_0$ . Thus,

$$|\theta_0| \leq |\theta| < \pi \quad (24)$$

The approximation,  $|\theta_0| \leq |\theta|$ , holds very well for all values of  $\theta_0$  examined thus far, the deviation being at most  $0.1^\circ$ .

2. The allowable range of  $\alpha$  is determined by eq 24. Substituting  $\theta$  of eq 22 into eq 24, we obtain

$$0 \leq |\alpha| < \arccos(|\theta_0|/\pi) \quad (25)$$

However, the upper limit of  $\alpha$  is actually determined by the magnitude of the distortion  $\delta$  (eq 18) allowed for the minor helix. A large value of  $\alpha$  can be obtained only by a large distortion of the minor helix, but the opposite is not true; i.e., both small and large values of  $\alpha$  can arise from large values of  $\delta$ . The upper limit of the calculated values of  $\alpha$  shown in Figures 4-6 is determined by the range taken for  $\Delta\phi$  and  $\Delta\psi$ . If these ranges were decreased, say to  $-5^\circ \leq (\Delta\phi, \Delta\psi) \leq 5^\circ$ , then only small values of  $\alpha$  would be allowed, e.g.,  $0 \leq \alpha \leq 50^\circ$  for  $\theta_0 = 10^\circ$ , and the distribution becomes narrower in accord

with the smaller deformation of the chain, as noted earlier.

3. The possible range of  $H$  (eq 20) is given by the allowed range of  $\alpha$  (eq 25), i.e.,

$$mh^* \geq H > (|\theta_0|/\pi)mh^* \quad (26)$$

However, the lower limit of  $H$  is determined actually by the maximum distortion allowed in the minor helix, as mentioned above.

4.  $R$  varies with  $\alpha$  as  $\sin 2\alpha$  (eq 23); thus, its maximum value arises at  $|\alpha| = 45^\circ$  (see Figure 6). The range of  $R$  is given by

$$0 \leq R \lesssim mh^*/2|\theta_0| \quad (27)$$

and a small value of  $\theta_0$  gives rise to a large value of  $R$  (see Figure 6).

It should be noted that the parameter  $\theta_0$  has not been discussed in this section. It is different in nature from the other parameters, since the absolute value of  $\theta_0$  (and also  $r$ , when it is a variable) depends on the reference atom chosen, while the other parameters are independent of which atom is chosen as the reference. This is the reason why  $\theta_0$  (and  $r$ ) do not appear in the above equations relating  $(\theta, H, R)$  to  $(\theta^*, h^*)$ .

As already mentioned, the distribution of the calculated points depends only on the helicity ( $\theta^*$  and  $h^*$ ) and on the magnitude of the distortion ( $\delta$ ) of the minor helix, but is not influenced by the dihedral angles, for a given  $\theta^*$  and  $h^*$ ; i.e., many values of  $\phi_i, \psi_i, \omega_i$ , and also bond lengths and bond angles, for a fixed  $m$ , can lead to the same value of  $\theta^*$  and  $h^*$ , but it is only the values of  $\theta^*$  and  $h^*$  that are primarily responsible in restricting the shape of the major helix. This follows from the test described above, in which  $\Delta\omega$  was taken as zero and as a variable, respectively. Therefore, the approximate relations presented in this section, and Figures 4-6, are applicable, in general, to any coiled-coil system no matter what the nature of the minor helix is or whether the geometry is treated as fixed or flexible. Thus, these relations are not restricted to  $\beta$  structures, but are equally applicable to  $\alpha$  helices, collagen structures, etc. However, the approximate relations are probably good only when the chain deformation (defined as in eq 18) is relatively small.

We have developed two independent relations (eq 19 and 21) among three parameters,  $\theta, H$ , and  $R$ , of the major helix for given values of  $\theta^*, h^*$ , and  $m$ . Therefore, only one of  $\theta, H$ , and  $R$  is an independent parameter (for fixed values of  $\theta^*, h^*$ , and  $m$ ) no matter how many variables,  $\Delta\phi_i, \Delta\psi_i$ , there are in the repeating unit; thus, if, say,  $R$  is given, then  $\theta$  and  $H$  are determined (approximately) by eq 19 and 21 (for given  $\theta^*, h^*$ , and  $m$ ). Of the two other parameters,  $\theta_0$  is the only independent one that is not restricted by  $\theta^*, h^*$ , and  $m$ , while  $r$  is determined by  $\theta^*$  and  $h^*$  (eq 9). Thus, in general, a coiled-coil structure, for a given averaged structure of the minor helix (and given value of  $m$ ), can be specified by two parameters, say  $R$  and  $\theta_0$ .

### III. Coiled-Coil Structures of Two-Stranded Antiparallel $\beta$ -Poly(L-alanine)

In section II, we discussed the general nature of coiled-coil structures for a single-stranded polypeptide chain. In this section, we will apply the method developed in this paper to a particular coiled-coil system, viz., that of two-stranded antiparallel  $\beta$  poly(L-alanine). The antiparallel chain arrangement is chosen here because it, rather than the parallel-chain arrangement, is observed in synthetic polyamino acids.<sup>21</sup> While most of the discussion pertains primarily to the backbone structure, we select the alanine residue (with a very small side chain) to simplify the energy calculations which are dealt with briefly later in this section. This simple coiled-coil system

may possibly serve as a model for the twisted  $\beta$  structure found in globular proteins.<sup>15</sup>

Assuming dyad symmetry perpendicular to the  $z$  axis (see Figure 1 of ref 20), the arrangement of the two-stranded antiparallel coiled coil (with a common major helix axis) can be deduced easily from a given coiled-coil structure of the single chain;<sup>11,18</sup> the second chain is obtained by a  $180^\circ$  rotation of the first chain around the  $z$  axis of the major helix and a successive  $180^\circ$  rotation about the  $x$  axis of the major helix (Figure 1). However, one degree of freedom [the relative translation of one chain with respect to the other along the  $z$  axis (denoted by  $\Delta z$ ; see ref. 22 for the precise definition of  $\Delta z$ )] remains in order to specify the antiparallel coiled coil, as well as the antiparallel straight (pleated sheet)  $\beta$  structure. The interchain interactions are altered as  $\Delta z$  varies, but  $\Delta z$  is restricted to a small range<sup>22</sup> to achieve optimal hydrogen bonding between chains, in the  $\beta$  structure. Thus, it is reasonable to treat  $\Delta z$  as a dependent, rather than as an independent, variable, with its value determined by the requirement that the H and O atoms of adjacent chains be in a hydrogen-bonding interaction at the same  $z$  coordinate. By imposing this restriction, the chain arrangement of the two-stranded coiled coil under investigation in this section is fully determined once the single-chain conformation is given.

The ten different conformations listed in Table I are again used as representative structures of the minor helix, from which two-stranded coiled-coil  $\beta$  structures will be constructed. These coiled coils, of both right- and left-handed minor helices, will be compared with the standard (straight) antiparallel  $\beta$  structure (conformation A of Table I). The chain arrangement of the two-stranded (straight) antiparallel  $\beta$  structure, constructed from a fixed single-chain conformation, is characterized by two parameters:<sup>22</sup> the chain separation,  $a/2$ , where  $a$  is the lattice constant<sup>20,22</sup> in the direction of the hydrogen bonds of the antiparallel  $\beta$  pleated-sheet structure; and the rotation of the individual chain about its own axis,  $z_{\text{rot}}$  (the third parameter,  $\Delta z$ , is treated in the manner described in the previous paragraph). For such an arrangement of two chains, the radius,  $R$ , of the coiled-coil  $\beta$  structure corresponds to  $a/4$  of the standard (straight)  $\beta$  structure, and the orientation angle  $\theta_0$  of the minor helix has the same meaning as  $z_{\text{rot}}$ .

As stated in section II, these two parameters ( $R$  and  $\theta_0$ ) are sufficient to specify the coiled-coil structure for a given set of values of  $(\phi^*, \psi^*)$  and  $m = 2$ . Thus, both the coiled-coil and straight  $\beta$  structures can each be described as a two-independent-parameter system. However, there is an important difference between them. In the straight  $\beta$  structure, the parameters  $a/4$  and  $z_{\text{rot}}$  are independent of the single-chain conformation whereas, in the coiled coil,  $R$  and  $\theta_0$  depend on the dihedral angles of the chains (i.e., on the deformation of the chains).

First, we will examine the relation between  $(R, \theta_0)$  and  $(\phi^*, \psi^*)$  for the single-chain conformation, and will show that it constitutes a severe restriction for formation of a coiled-coil  $\beta$  structure. Then we will treat the two-stranded structure. Considering the system as a two-parameter one, it is reasonable to choose  $\Delta\phi$  and  $\Delta\psi$  of eq 16 as the independent variables, and fix  $\omega$  at  $180^\circ$  ( $\Delta\omega = 0^\circ$ ), and use standard (rigid) geometry. The variable range of  $\Delta\phi$  and  $\Delta\psi$ , for a given value of  $(\phi^*, \psi^*)$ , will be limited again to  $-20$  to  $20^\circ$ , as in section II. The possible range of  $R$ , for each value of  $(\phi^*, \psi^*)$ , is already shown in Figure 6. However, we are now interested in a more restricted range of  $R$ , viz., that around  $2.5 \pm 0.5 \text{ \AA}$  since the chain separation ( $a/2$ ) cannot be expected to deviate much from that of the straight antiparallel  $\beta$  structure (with optimum hydrogen bonding), for which  $a \sim 9.50 \text{ \AA}$ .<sup>20</sup> If we plot a set of contours of constant  $R$  (not shown here) on a  $\Delta\phi$ - $\Delta\psi$  grid, for a given value of  $\theta_0$ , the value of  $R$  is zero at the origin

**Table II**  
Geometrical Limitations for the Coiled-Coil  $\beta$  Structure

	$\theta_0$ , deg	Is $R \sim$ $2.5 \text{ \AA}$ ?	Allowable range <sup>a</sup> of $\theta_0$ , deg (for $R \sim 2.5 \text{ \AA}$ )	Is H bonding good? <sup>b</sup>
A	0	Yes	All values	Yes
B <sub>L</sub>	10	Yes	All values	Yes
C <sub>L</sub>	20	Yes	85–155	No
D <sub>L</sub>	40	Yes	115–135	No
E <sub>L</sub>	60	Yes	120–130	No
F <sub>L</sub>	80	No		
B <sub>R</sub>	–10	Yes	All values	Yes
C <sub>R</sub>	–20	Yes	All values	Yes
D <sub>R</sub>	–40	Yes	85–155	No
E <sub>R</sub>	–60	Yes	110–140	No
F <sub>R</sub>	–80	No		

<sup>a</sup> Only positive values of  $\theta_0$  are listed, but the range is symmetrical to include the corresponding negative values. <sup>b</sup> Good hydrogen bonding means:  $R \sim 2.5 \text{ \AA}$  and  $\theta_0 \sim 70^\circ$ .

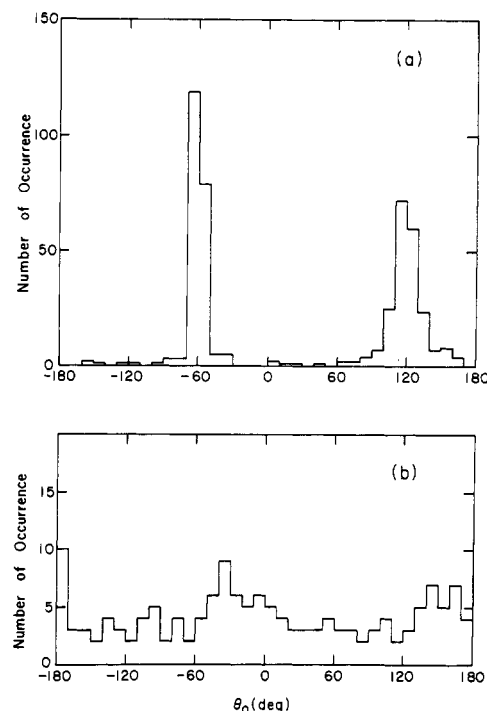


**Figure 8.** Distribution of calculated values of  $\theta_0$  for  $\theta_0 = 10^\circ$ . (a) for  $\Delta\phi, \Delta\psi$  in the range from  $-20$  to  $20^\circ$  (in  $2^\circ$  intervals), and  $\Delta\omega = 0^\circ$ ; (b) for  $\Delta\phi, \Delta\psi, \Delta\omega$  in the range  $-10$  to  $10^\circ$  (in  $4^\circ$  intervals).

( $\Delta\phi = \Delta\psi = 0^\circ$ ) and increases on concentric oval-shaped contours as the distance from the origin increases. The contour line for  $R = 2.5 \text{ \AA}$  varies with the value of  $\theta_0$  of Table I; also, the contour patterns for, say, conformations B<sub>L</sub> ( $\theta_0 = 10^\circ$ ) and B<sub>R</sub> ( $\theta_0 = -10^\circ$ ) are not the same because they are not mirror images, as already pointed out in section II. In general, the  $2.5 \text{ \AA}$  contour lies near the origin for small values of  $|\theta_0|$  and moves out of the range chosen for  $\Delta\phi$  and  $\Delta\psi$  for  $|\theta_0| = 80^\circ$  (i.e., for conformations F<sub>L</sub> and F<sub>R</sub>); this behavior is also evident in Figure 6. The maximum value of  $R$  obtained for both the F<sub>L</sub> and F<sub>R</sub> conformations is about  $2.0 \text{ \AA}$ ; hence, these conformations would never be able to form a coiled-coil  $\beta$  structure with optimum hydrogen bonding (see column 3 of Table II).

The parameter  $\theta_0$  depends on the reference atom chosen,



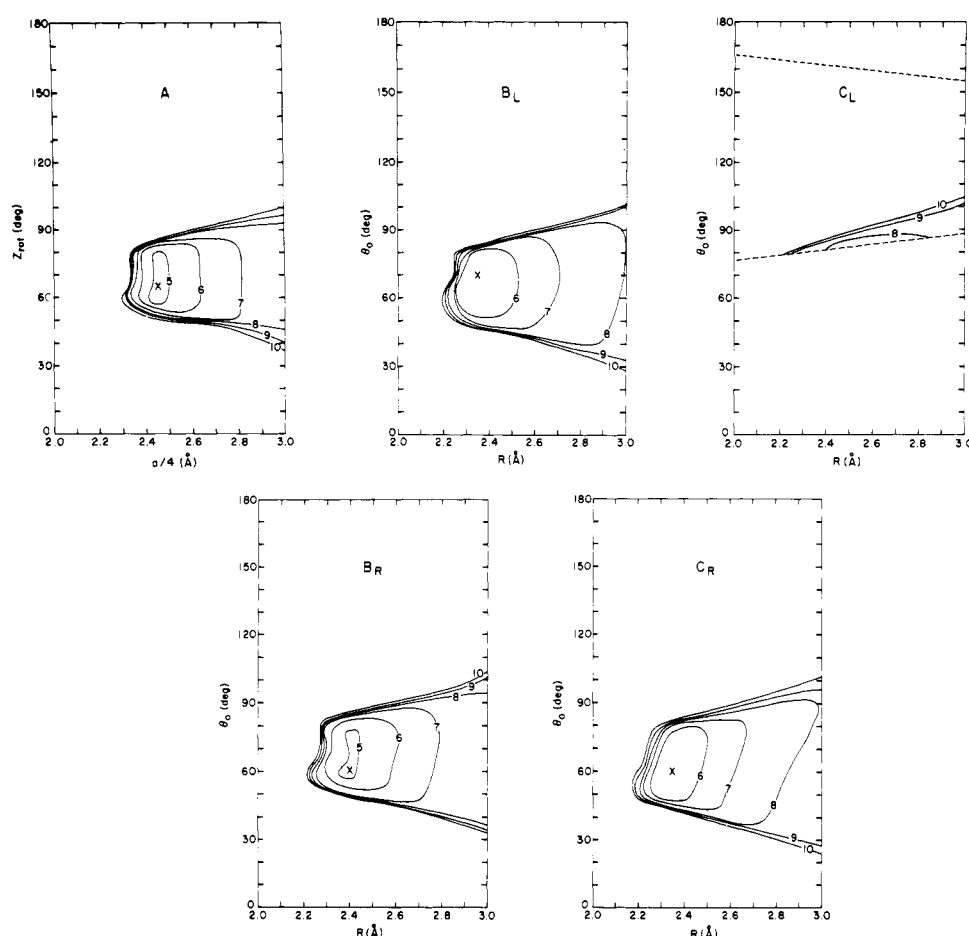


**Figure 9.** Energy contour maps for two-stranded antiparallel  $\beta$  structures of poly(L-alanine), for the averaged minor helices  $B_L$ ,  $C_L$ ,  $B_R$ , and  $C_R$  (Table I) and for the corresponding straight  $\beta$  structure formed from two chains, each of which had conformation A (Table I). The contours represent the total energy per two residues (in kcal/mol) on an  $R$ - $\theta_0$  map for coiled coils, and on an  $a/4$ - $z_{rot}$  map for the straight  $\beta$  structure. The X indicates the position of lowest energy. For  $C_L$ , the region between the dashed lines is the only one obtained in the given range of  $\Delta\phi$  and  $\Delta\psi$  (i.e.,  $-20$  to  $20^\circ$ ).

and we will select the  $C^\alpha$  of the first residue of the repeating unit (of two residues) as the reference atom. Then, since  $m = 2$ , the value of  $\theta_0$  for the  $C^\alpha$  atom of the second residue should be close to  $\theta_0 + 180^\circ$ , as pointed out in section I. Of course, it is arbitrary, in a homopolymer, as to which residues are designated as the "first" and "second" in the repeating unit. Thus,  $\theta_0$  is twofold; i.e.,  $\theta_0$  and (approximately)  $\theta_0 + 180^\circ$  correspond to the same structure.

In contrast to the  $R$  contours on a  $\Delta\phi$ - $\Delta\psi$  grid, the contour lines of constant  $\theta_0$  on such a grid (not shown here) radiate out from the origin in various directions (the origin is a point of discontinuity; i.e.,  $\theta_0$  has no meaning for a simple helix, for which  $\Delta\phi = \Delta\psi = 0^\circ$ ). However, the distribution of the calculated values of  $\theta_0$  on such a grid is found to indicate an overwhelmingly large preference for values around  $\theta_0 \sim 120^\circ$  (or  $\theta_0 \sim -60^\circ$ ), and this pattern is essentially independent of the value of  $\theta_0$  (if  $\Delta\omega = 0^\circ$ ). One example of such a distribution (for  $\theta_0 = 10^\circ$ ) is shown in Figure 8a, where the number of calculated points (in  $2^\circ$  intervals for both  $\Delta\phi$  and  $\Delta\psi$ ) in each range of  $\theta_0$  is plotted against  $\theta_0$ . The preference for  $\theta_0 \sim 120^\circ$  (or  $-60^\circ$ ) is clear from Figure 8a. Values of  $\theta_0$  differing markedly from  $120^\circ$  (for  $-60^\circ$ ) rarely occur, and are found only in a small region along the diagonal line  $\Delta\phi \approx \Delta\psi$  on the  $\Delta\phi$ - $\Delta\psi$  grid.

These results for  $\theta_0$  may be attributed to the conditions imposed here, viz.,  $m = 2$  and  $\Delta\omega = 0^\circ$ . This can be seen by recognizing that there are four variable dihedral angles in the repeating unit,  $\phi_1$ ,  $\psi_1$ ,  $\phi_2$ , and  $\psi_2$ , but, with a planar trans

peptide conformation, the N- $C^\alpha$  bond for  $\phi_1$  (for  $\omega_1$  fixed at  $180^\circ$ ) is almost parallel to the  $C^\alpha$ -C' bond for  $\psi_2$ , and also the  $C^\alpha$ -C' bond for  $\psi_1$  is nearly parallel to the N- $C^\alpha$  bond for  $\phi_2$ . Furthermore,  $\phi_1$  and  $\phi_2$ , and  $\psi_1$  and  $\psi_2$ , are related by only one parameter, viz.,  $\Delta\phi$  and  $\Delta\psi$ , respectively (eq 16), so that only one direction of the chain [i.e.,  $120^\circ$  (or  $-60^\circ$ ) of Figure 8a] can be affected by variation of these dihedral angles. This explanation has been tested by inclusion of  $\Delta\omega$  as a variable, and verified as shown in Figure 8b; i.e., if  $\omega$  varies, there is no preferred value of  $\theta_0$  (in contrast to Figure 8a), and a coiled coil can be obtained for any value of  $\theta_0$ .

Thus, the severe restriction for the orientation of the minor helix (shown in Figure 8a) is a consequence of the restrictions that  $m = 2$  and  $\omega$  is fixed at  $180^\circ$ . However, since  $\omega$  generally does have the value  $180^\circ$ , except in strained molecules such as cyclic oligopeptides, we will maintain the restrictions of  $m = 2$  and  $\Delta\omega = 0^\circ$  in our further discussion of the coiled-coil  $\beta$  structure.

We now consider the combined ranges of  $\theta_0$  and  $R$  by seeking the allowed range of  $\theta_0$  when  $R \sim 2.5$  Å. Since the contour line for  $R = 2.5$  Å varies with the value of  $\theta_0$ , this range of  $\theta_0$  differs for different values of  $\theta_0$ . From an examination of the  $\theta_0$  contours and the  $R = 2.5$  Å contour on a  $\Delta\phi$ - $\Delta\psi$  grid, it appears that all values of  $\theta_0$  are allowed if  $|\theta_0|$  is small; i.e., if  $|\theta_0|$  is small, the  $R = 2.5$  Å contour is a small ellipsoid centered at the origin, and the  $\theta_0$  contours (which radiate from the origin) cross this ellipsoid for all values of  $\theta_0$ . On the other hand, for large  $|\theta_0|$ , the  $R = 2.5$  Å contour is so far from the

origin that only a portion of it lies within the chosen range of  $\Delta\phi$  and  $\Delta\psi$ ; thus, only the contours near  $\theta_0 \sim 120^\circ$  can intersect the  $R = 2.5 \text{ \AA}$  contour in this range of  $\Delta\phi$  and  $\Delta\psi$ , and hence values of  $\theta_0$  around  $120^\circ$  are the only allowed ones. The ranges of  $\theta_0$  for each value of  $\Theta_0$  of Table I, for  $(\Delta\phi, \Delta\psi)$  in the range from  $-20$  to  $20^\circ$ , are listed in Table II. Considering that good hydrogen bonding occurs for  $\theta_0 \sim 70^\circ$ ,<sup>22,23</sup> we can conclude that, on the basis of geometric criteria alone, only three conformations ( $B_L$ ,  $B_R$ , and  $C_R$ ) can form a coiled-coil  $\beta$  structure. Of course, energy considerations (including those involving the side chains) may place a further limitation on the possible coiled-coil  $\beta$  structures that can exist.

Having considered the single-chain coiled-coil  $\beta$  structure, we now turn to the two-stranded coiled-coil  $\beta$  structure of poly(L-alanine). Here, we will consider not only the geometrical criteria, but also the conformational energies, for formation of coiled-coil structures. For purposes of computation, a chain length of 14 residues was taken for each strand, and the side-chain dihedral angle  $\chi$  of L-alanine was kept at  $60^\circ$ .<sup>24</sup> The total conformational energy was calculated at each point on an  $(R, \theta_0)$  grid;  $R$  was varied from 2.0 to 3.0  $\text{\AA}$  in 0.05- $\text{\AA}$  steps, and  $\theta_0$  from 0 to  $180^\circ$  (in the allowed ranges of Table II) in  $5^\circ$  steps. At each  $(R, \theta_0)$  point, values of  $\Delta\phi$  and  $\Delta\psi$  for a given  $(\phi^*, \psi^*)$  from Table I were computed with the use of eq 13–15 to obtain the two-stranded antiparallel coiled-coil  $\beta$  structure (see Appendix B for details). Incidentally, the other parameters of the major helix ( $\Theta$  and  $H$ ) were also computed from the values of  $(\Delta\phi, \Delta\psi)$ , using eq 11 and 12. However, their values were almost constant in the range of  $R$  considered here, as expected from the approximate relations discussed in section II. The energy functions<sup>19</sup> used here included nonbonded, electrostatic, and hydrogen-bonding contributions. The total energy per two residues (i.e., per repeating unit) was calculated by summing all pairwise interactions between the atoms of the central two reference residues and all other atoms in the system (28 residues in total). The total energy is expressed in terms of the intra-chain energy,  $E_{\text{INTRA}}$ , for a single strand of poly(L-alanine), and the interaction energy between the two chains,  $E_{\text{INTER}}$ ,<sup>22</sup> both of which were calculated from the same component energies mentioned above (and expressed as an energy per two residues).

Figure 9 shows the energy contour maps for averaged conformations  $B_L$ ,  $B_R$ , and  $C_R$  and, for comparison, a map for  $C_L$  which is a geometrically restricted structure, and a map for A which is the straight antiparallel  $\beta$  structure. It is clearly seen that only the region  $\theta_0 \sim 70^\circ$  is low in energy and that, outside of this region, the energy increases rapidly because of interatomic overlaps, especially side chain–side chain overlaps. Therefore, the geometrically favorable region around  $\theta_0 \sim 120^\circ$  (which is enclosed between dashed lines for  $C_L$ ) is always of high energy. The behavior shown for  $C_L$  is similar to that for the other averaged conformations,  $D_L$ ,  $E_L$ ,  $D_R$ , and  $E_R$  (whose energy contour maps are not shown here), as expected from their  $\theta_0$  ranges shown in Table II.

For those structures with a fully allowed (geometrical) range of values of  $\theta_0$ , viz.,  $B_L$  which forms a right-handed major helix,  $B_R$  and  $C_R$  which form left-handed major helices, and A which is the straight  $\beta$  structure, there is essentially no difference in the energies at the lowest point on each map (see Table III). It can be seen that the single-chain energy,  $E_{\text{INTRA}}$ , the interchain interaction energy,  $E_{\text{INTER}}$ , and the total energy are similar in all four cases. Thus, this computation indicates that there is no preference for either right- or left-handed coiling. This result was extended by replacing one alanyl residue of the repeating unit by a bulkier residue, L-valine, i.e., by considering the two-stranded regularly repeating copolymer  $(\text{Ala-Val})_n$ . The result was similar; i.e., the interchain interactions in this copolymer did not lead to a preference for right-

or left-handed coiling, although the low-energy region (analogue of Figure 9) was narrower in the  $\theta_0$  direction than for poly(L-alanine).

The conclusion from the energy calculations is almost the same as that deduced only from geometrical considerations (Table II). Only slowly winding coiled coils of the two-stranded antiparallel  $\beta$  structure are geometrically allowed, and the straight and right- and left-handed coiled coils have almost the same energy. However, the straight  $\beta$  structure would be expected to have a higher entropy because variations in the dihedral angles are independent of variations in the lattice variables  $a/2$  and  $z_{\text{rot}}$  (see ref 25 for further discussion of various entropy contributions in a multistranded structure). On the other hand, even a small fluctuation in the dihedral angles can give rise to significant (and unallowed) changes in the values of  $R$  and  $\theta_0$  of a coiled-coil system. In short, the coiled-coil system is entropically less stable, so that some other energetic factor would be required to stabilize the coiled-coil form of a  $\beta$  structure.

The model of the coiled-coil  $\beta$  structure used here was based on several assumptions: a two-stranded antiparallel arrangement of chains with dyad symmetry, equivalence of pairs of hydrogen bonds from one two-residue repeating residue to another ( $m = 2$ ), planar trans peptide groups, and only a limited number of conformations of the averaged minor helix were examined. This model was chosen to try to account for the twisted  $\beta$  structures observed in globular proteins.<sup>15</sup> However, with the above assumptions in mind, we must conclude that this model is not applicable to the real  $\beta$  structures in globular proteins. Finally, we conclude further that two-stranded antiparallel  $\beta$  structures of any protein or synthetic polypeptide are unlikely to form a coiled coil with regular hydrogen bonding.

#### IV. Discussion of Twisted $\beta$ Structures in Globular and Fibrous Proteins

Chothia<sup>15</sup> has pointed out that the  $\beta$ -sheet structures observed in various globular proteins are twisted rather than straight as originally proposed by Pauling and Corey<sup>26</sup> and, moreover, the twist is always right handed. It is not clear whether the model used by Chothia<sup>15</sup> is intended to be a coiled coil or an assembly of straight chains which cross one another. Since he made no mention<sup>15</sup> about the feature of a coiled coil, about the number of residues in a repeating unit, nor about the distortions  $(\Delta\phi_i, \Delta\psi_i)$  of the dihedral angles, we will treat his model here as one in which straight chains cross one another. His model may be compared with the concepts used in the present paper. Each straight chain of his model may be interpreted as an averaged structure of a minor helix, and the twist of the hydrogen-bonding arrangement (when viewed along the direction of the polypeptide chain) may be expressed by the rotation per two residues ( $\theta_0$ ) because the pair of hydrogen bonds occurs at every two residues. Thus, the observed<sup>15</sup> "right-handed twist" of the major helix implies that the minor helix is left handed (see Table I). Chothia's assembly of crossing (straight) chains would then be analogous to the multistranded coiled coil [the two chains in the two-stranded coiled coil cross each other at an angle of  $2\alpha$  when viewed in a direction perpendicular to the  $z$  axis]. This analogy holds because the coiled-coil structure can be approximated by straight (minor) helices over a relatively short range along the polypeptide chain.

The observed  $\beta$  structures in globular proteins usually are short, say four to six residues long, so that the difference between the coiled-coil model and Chothia's crossing model may be negligible. However, the crossing model cannot be used for the energy calculation because the residues in different positions along the chain are not equivalent to each other; i.e.,

**Table III**  
**Energies and Geometrical Parameters of the Two-Stranded Coiled-Coil Antiparallel  $\beta$  Structure of Poly(L-alanine) at the Point of Lowest Energy<sup>a,b</sup>**

	<i>E</i> , kcal/mol/two residues			<i>R</i> , Å	$\theta_0$ , deg	$\Delta z$ , <sup>c</sup> Å	$\Theta$ , deg	<i>H</i> , Å	$\alpha$ , deg	$\Delta\phi$ , deg	$\Delta\psi$ , deg
	Total	INTRA	INTER								
A <sup>d</sup>	4.825	9.091	-4.265	2.45	65	0.008					
B <sub>L</sub>	5.136	9.284	-4.148	2.35	70	-0.036	10.0	6.86	3.4	-5.1	-4.1
B <sub>R</sub>	4.831	9.031	-4.200	2.40	60	-0.035	-10.1	6.85	-3.5	-3.1	-2.6
C <sub>R</sub>	5.326	9.395	-4.069	2.35	60	-0.104	-20.1	6.78	-6.9	-9.5	-7.7

<sup>a</sup> See Table I for the values of the other parameters ( $\phi^*$ ,  $\psi^*$ , etc.). <sup>b</sup> The data for C<sub>L</sub> are omitted since its energy is much higher ( $E_{\text{total}} \sim 7$  kcal/mol/two residues). <sup>c</sup> Obtained by imposing the restriction that the H and O atoms in a hydrogen bond have the same *z* coordinate. <sup>d</sup> Not a coiled coil.

the inter-chain interactions vary with distance from the crossing point of the chains. This is one of the reasons that the coiled-coil model (for which the residues are equivalent along the chain) was chosen, in the present study, for the energy calculation. Even though Chothia<sup>15</sup> did not carry out any energy calculations, he suggested (on the basis of relative areas on a  $\phi$ - $\psi$  diagram) that the preference for a right-handed twist arises from an entropic factor rather than from the interchain interaction energy. Our energy calculations described in section IV support his suggestion, but only to the extent that we find no *energetic* preference for either a right- or left-handed coiled coil.

However, the coiled-coil model chosen in the present study is really not suitable to account for the wide distributions of the observed values of  $\phi$  and  $\psi$  in  $\beta$  structures,<sup>15</sup> since the  $\phi$ ,  $\psi$  region (other than that in the narrow range of  $\theta^*$  between the lines for 170 and  $-175^\circ$  in Figure 3) cannot lead to energetically favorable coiled coils, as shown in section III. The inapplicability of our model may be attributed to the restricting assumptions adopted (i.e., the assumption that  $m = 2$  implies that all of the pairs of hydrogen bonds are equivalent in every two residues), and this may not be true for the  $\beta$  structures in globular proteins which have non-regular amino acid sequences [i.e., in a specific sequence copolymer (i.e., a protein) the condition  $m > 2$  probably holds]. This nonregularity of the actual twisted  $\beta$  structure may be required to provide a wide distribution of  $\phi$ ,  $\psi$  to stabilize the system entropically; without such an entropic stabilization, the coiled coil would be less stable than the straight  $\beta$  structure, as discussed in section III. The crossing model of Chothia<sup>15</sup> may be good enough for treating the *geometry* of short  $\beta$  structures, but longer structures would have to be treated as coiled coils (probably with  $m > 2$ ).

Another type of twisted  $\beta$  structure has been proposed for feather keratin.<sup>27</sup> However, their model is not a coiled coil of unbroken polypeptide chains, but is an assembly of separate  $\beta$  sheets, twisted about a common (straight) major helix axis. Thus, we cannot compare our model of section III to theirs, but simply point out the following fact. Fraser et al.<sup>27</sup> calculated the intensity transform, assuming a left-handed twist for the major helix, and obtained good agreement with the observed intensities of the x-ray diffraction pattern. However, since the right-handed twist occurs in the  $\beta$  structures of globular proteins,<sup>15</sup> it is hard to accept the assumption that the twist of the major helix in feather keratin is left handed.

## V. Coiled Coils of $\alpha$ Helices

Coiled-coil models of  $\alpha$ -keratin have been proposed by Crick<sup>4</sup> (a two- and a three-stranded model) and by Pauling and Corey<sup>28</sup> (a seven-stranded model). Later, Crick's model, or a variation<sup>5</sup> of it, was accepted<sup>5</sup> as the more plausible one for  $\alpha$ -keratin; viz., a three-stranded model with a value of  $m$

$= 7$  was taken for  $\alpha$ -keratin.<sup>5</sup> The value of  $m = 7$  was accounted for by Crick<sup>4</sup> on the basis of packing interactions between the side chains of adjacent helices in the coiled-coil structure.

Instead of attributing the existence of coiled-coil structures of  $\alpha$  helices to packing interactions of side chains, we will show that, by using the approximate relations presented in section II, we can account for the existence of coiled coils on the basis of the geometrical properties of the backbone. Of course, energetic considerations (including interactions involving side chains) will determine which of the geometrically allowed *backbone* structures is most stable.

Taking the right-handed  $\alpha$  helix ( $\theta^* = 100^\circ$ ,  $h^* = 1.5$  Å) as the averaged structure of the minor helix, the values of  $\theta$ ,  $\Theta_0$ , and the maximum value of  $R$  ( $R_{\text{max}}$ ), given by eq 27, were calculated for various values of  $m$  (Table IV). It can be seen that all values of  $\theta$  are positive, in accordance with the right handedness of the minor helix ( $\alpha$  helix), while the values of  $\Theta_0$  are positive or negative depending on the value of  $m$ . The signs of  $\Theta$ , which is always that of  $\Theta_0$  according to eq 22, imply that *both* right- and left-handed major helices can be formed despite the fact that the minor helix is always right handed.

The values of  $R_{\text{max}}$  listed in Table IV are only approximate ones, because they were computed from the approximate eq 27. However, they are exact enough to provide a measure of the likely values of  $m$  for forming possible coiled coils. From model building, Crick<sup>4</sup> gave the values of  $R$  as 5.2 and 6.0 Å for the two- and three-stranded coiled-coil structures, respectively, of  $\alpha$  helices. Thus, we may expect to obtain multistranded (i.e., two- and three-stranded) coiled coils for values of  $m$  for which  $R_{\text{max}} > 5.2$  and 6.0 Å, respectively, i.e., for  $m = 7, 11, 14$ , and 15 (the values of  $R_{\text{max}}$  for other values of  $m$  are so small that atomic overlaps between  $\alpha$ -helical chains would occur);  $m = 10$  is impossible for the three-stranded coiled coil, and may be marginal for the two-stranded one because a large deformation is required to attain a value of  $R$  close to  $R_{\text{max}}$  [the coiled-coil models proposed thus far<sup>2-4</sup> have  $\alpha$  values of  $10$ – $20^\circ$ , whereas values of  $R$  close to  $R_{\text{max}}$  correspond to values of  $\alpha$  near  $45^\circ$  (see Figure 6), for which a larger deformation ( $\delta$ ) is required]. Thus, it appears that  $m = 7$  is the smallest value of  $m$  for formation of multistranded (two or three stranded) coiled coils of  $\alpha$  helices. Of the other three values of  $m$ ,  $m = 14$  is essentially the same as  $m = 7$  (except for slight variations in  $\phi_i$  and  $\psi_i$  in a seven-residue repeating unit compared to a 14-residue one); the averaged minor helix is the same for both  $m = 7$  and  $m = 14$ , but  $\Theta_0$  for  $m = 14$  is twice that for  $m = 7$ . The case of  $m = 11$  is interesting in that it gives a right-handed major helix of the same value of  $|\Theta_0|$  as that for  $m = 7$ .

It should be noted that the choices of  $m = 7, 11, 14$ , and 15 are based solely on backbone geometrical criteria. However, energetic considerations (arising from specific sequences of amino acids, such as the alternate occurrence of polar and

**Table IV**  
Estimated Values of  $R_{\max}$  of Coiled Coils of  $\alpha$  Helices<sup>a</sup> for  
Different Values of  $m$

$m$	$n$	$\theta$ , <sup>b</sup> deg	$\Theta_0$ , <sup>c</sup> deg	$R_{\max}$ , <sup>d</sup> Å
2	1	180	-160	0.5
3	1	120	-60	2.1
4	1	90	40	4.3
5	1	72	140	1.5
6	2	120	-120	2.1
7	2	103	-20	15.0
8	2	90	80	4.3
9	2	80	180	2.1
10	3	108	-80	5.4
11	3	98	20	23.6
12	3	90	120	4.3
13	4	111	-140	4.0
14	4	103	-40	15.0
15	4	96	60	10.7

<sup>a</sup>  $\theta^* = 100^\circ$  and  $h^* = 1.5$  Å. <sup>b</sup> From  $\theta = 2n\pi/m$ . <sup>c</sup> From eq 17. <sup>d</sup> From eq 27.

nonpolar residues, as demonstrated by Fraser and MacRae<sup>29</sup>) can place a further limitation on the actual values of  $m$  that are observed, but energy criteria can select only from among those values of  $m$  already allowed by geometrical considerations.

It can also be seen in Table IV that a large value of  $R_{\max}$  occurs only when  $\theta$  is close to the value of  $\theta^*$  ( $100^\circ$ ). Hence, as pointed out by Pauling and Corey,<sup>28</sup> a small change in the value of  $\theta^*$  (which may occur on occasion) will cause a large change in the values of the parameters of the major helix; e.g., when  $\theta^* = 101.5^\circ$ , the value of  $\Theta_0$  becomes  $-10^\circ$ , and  $R_{\max}$  is doubled, for  $m = 7$ . In general, the experimental determination of the parameters of the major helix may become less accurate as  $m$  increases (Figures 5 and 6 are normalized by the factor  $m$ , and the absolute deviations from the solid curves become large as  $m$  increases).

## VI. Concluding Discussion

We summarize here the main points of the foregoing treatment of coiled coils.

1. Five independent parameters are generally required to specify a single-stranded coiled coil (for a given value of  $m$ ). Of these, the major helix is characterized by the three parameters  $\Theta$ ,  $H$ , and  $R$ , and the other two parameters,  $\theta_0$  and  $r$ , determine the position of the reference atom ( $A_{jm}$ ) with respect to the curved axis of the minor helix (see section I).

2. The minor helix is defined, in the rotating frame, by the parameters  $\theta$  and  $r$  (Crick's method<sup>9</sup>). We also characterize the minor helix in another way, by introducing the concept of the averaged structure of the minor helix, with the parameters  $\theta^*$  and  $h^*$ . Although, the averaged structure of the minor helix is an approximation of the real minor helix, its advantage is that it provides an intuitive image of the minor helix.

3. Furthermore, the concept of the averaged structure of the minor helix turns out to be very important, since the parameters  $\theta^*$  and  $h^*$  (or, more directly,  $\Theta_0$  and  $mh^*$ ) are related to the shape of the major helix, i.e., to  $\Theta$ ,  $H$ , and  $R$ . When a simple (minor) helix is specified by  $\theta^*$  and  $h^*$  (together with the value of  $m$ ), the possible range of the parameters  $\Theta$ ,  $H$ , and  $R$  of the major helix is strongly restricted, and can be estimated easily (see section II). This restriction, which was deduced in the analysis of a single-stranded coiled-coil  $\beta$  structure, is expressed in a general form (see second paragraph following eq

27), and is applicable to the  $\alpha$ -helical coiled coil (see section V).

4. All the parameters of the coiled coil are combined with the backbone dihedral angles under the assumption of fixed bond lengths and bond angles; i.e., the values of the parameters of the coiled coil can be calculated from the given values of the backbone dihedral angles (see section I).

5. The reverse process, i.e., the calculation of the backbone dihedral angles from the given values of the parameters of the coiled coil, is generally more difficult, and a unique solution is not obtained if the number of backbone dihedral angles in the repeating unit is larger than the number of given parameters of the coiled coil.

In this respect, it is worth pointing out that the procedure of Ramachandran et al.<sup>30</sup> and Traub et al.<sup>16,31</sup> is an attempt to carry out this reverse process. They tried to fit the backbone conformation of collagen to the experimental values of  $\Theta$ ,  $H$ , and  $R_A$  (the radius of the major helix, with respect to the reference atom A) by varying the backbone dihedral angles and also the bond angles, keeping the bond lengths fixed. Their method,<sup>16,30,31</sup> which is difficult to understand because of the introduction of many auxiliary parameters, is not analytical but a trial and error one with the use of a computer.

The approach in this reverse process becomes feasible with the use of the relations between the averaged structure of the minor helix and the major helix, developed in section II. These relations are approximate, but good enough to define the coiled-coil structure so that the effective number of independent parameters is reduced to two, viz.,  $R$  and  $\theta_0$ , with the values of  $\phi^*$ ,  $\psi^*$ , and  $m$  fixed. Thus, the values of  $\Delta\phi$  and  $\Delta\psi$  can be computed uniquely from the given values of  $R$  and  $\theta_0$  (see section III and Appendix B).

6. Multistranded coiled coils (with a common  $z$  axis) can be constructed by specifying a symmetry relation for the arrangement of the chains (e.g., the twofold screw symmetry of the double-stranded  $\beta$  structure in section III, or the threefold screw symmetry of the triple-stranded structure of collagen). However, some of the multiple-stranded structures cannot exist because of the geometrical restrictions discussed in this paper (and also because of energy restrictions discussed elsewhere<sup>11</sup> for collagen). From the point of view of the geometrical restrictions, the value of  $R_{\max}$ , estimated from the given values of  $\theta^*$ ,  $h^*$ , and  $m$ , can be used as a necessary condition for the existence of multistranded coiled coils (see Tables II and IV). The value of  $\theta_0$  (together with the imposed symmetry relation) determines the mutual orientation of the chains, especially the direction of the hydrogen bonds between the chains (see Table II). This factor may be useful, for example, in distinguishing between the different hydrogen-bonding arrangement in the several models of collagen. However, the orientation angle,  $\theta_0$ , has never been discussed in the description of collagen models. This may be the reason that it is sometimes difficult to understand the differences between various collagen models. For example, the collagen I and II models,<sup>3</sup> which are described as having different hydrogen-bond arrangements,<sup>3</sup> have never been distinguished in terms of the coiled-coil parameters. The difference between the two models may be attributed simply to different values of  $\theta_0$  (because of the different hydrogen-bond arrangements), with the remaining parameters ( $\Theta$ ,  $H$ ,  $R$ ,  $r$ ) being essentially the same for both models.

7. For the double-stranded coiled coil of the antiparallel  $\beta$  structure, the geometrical criteria are fully confirmed by energy calculations in the sense that conformations B<sub>L</sub>, B<sub>R</sub>, and C<sub>R</sub> form coiled coils with good hydrogen bonds (see Tables II and III). The geometrical restriction on coiled coiling was found to be very severe under the assumption that the two hydrogen bonds in every second residue are equivalent (i.e.,

$m = 2$ ). Hence, an ideal coiled-coil  $\beta$  structure (i.e., with  $m = 2$ ) would not be expected to exist, and the twisted (right handed)  $\beta$  structure observed in globular proteins<sup>15</sup> is probably the consequence of a deformation of the coiled coil (i.e., with  $m > 2$ ), from the viewpoint of the coiled-coil model (see section IV).

**Acknowledgment.** We are indebted to Martha H. Miller for helpful discussions about the structure of collagen.

#### Appendix A. Derivation of the Relation between Coiled-Coil Parameters and Backbone Dihedral Angles

In using the Sugeta-Miyazawa procedure, we must express the coordinates of *all* atoms  $A_{jm}$  in a local coordinate system on the polypeptide chain, the origin of which is taken, as usual, at the atom  $A_0$ . Once the position vector  $\vec{A_0Q_0} (= -\mathbf{r})$  is already expressed in terms of  $\phi^*$  and  $\psi^*$  (eq 10 in the text), the position of all  $Q_{jm}$  ( $j \neq 0$ ) is obtainable by a transformation of the vector  $\vec{A_0Q_0}$  along the polypeptide chain with the use of the dihedral angles  $\phi_i$  and  $\psi_i$  of eq 7; this is the usual transformation from one residue to another along the polypeptide chain in order to express all atoms (including the dummy atoms  $Q_{jm}$ ) in a common coordinate system.

Then, the vectors joining these reference "atoms", i.e., the vectors  $\mathbf{b}$  and  $\mathbf{d}$  in Figure 2a, are also functions of the dihedral angles ( $\phi_i, \psi_i$ ). The vectors  $\mathbf{a}$  and  $\mathbf{c}$  of Figure 2a are given as

$$\mathbf{a}_i = \mathbf{b}_{i-1} - \mathbf{b}_i \quad (i = 0, 1, \dots)$$

and

$$\mathbf{c}_i = \mathbf{d}_{i-1} - \mathbf{d}_i \quad (i = 0, 1, \dots)$$

The lengths  $a, b, c$ , and  $d$  of these vectors are also functions of the dihedral angles. Equations 11, 12, and 13 in the text correspond to eq 15, 18, and 16 of Sugeta and Miyazawa,<sup>14</sup> and their method is applied twice, once to the simple helix consisting of reference atoms  $A_{jm}$  to obtain eq 11 and 12, and once to the simple helix consisting of "atoms"  $Q_{jm}$  to obtain eq 13;  $\theta, \mathbf{a}_0, \mathbf{a}_1, \mathbf{b}_0$ , and  $H$  for reference atom  $A_{jm}$  correspond to their  $\theta, \mathbf{C}, \mathbf{C}', \mathbf{B}$  and  $d$ , respectively, and  $R, \theta$ , and  $\mathbf{c}$  for reference "atom"  $Q_{jm}$  correspond to their  $\rho, \theta$ , and  $\mathbf{C}$ , respectively. Equations 14 and 15 for the orientation angle  $\theta_0$  are derived directly from Figure 2a. The details are shown in the Sugeta-Miyazawa paper.

#### Appendix B. Calculation of $\Delta\phi$ and $\Delta\psi$ from a Given Set of $(R, \theta_0)$ for Fixed Values of $\phi^*$ and $\psi^*$

The coiled-coil  $\beta$  structure in section III is, fortunately, a two-variable system (i.e.,  $\Delta\phi$  and  $\Delta\psi$ ), so that  $\Delta\phi$  and  $\Delta\psi$  can be determined uniquely from a given set of  $(R, \theta_0)$  for fixed values of  $\phi^*$  and  $\psi^*$ . However,  $\Delta\phi$  and  $\Delta\psi$  cannot be obtained directly from an analytical solution of eq 13-15. Instead, these equations have to be solved numerically as follows.

First, a particular set of  $(\Delta\phi, \Delta\psi)$  must be chosen as the

initial values for the given values of  $R, \theta_0$ , and  $\phi^*, \psi^*$ . Then the values of the following functions are calculated:

$$f_1 = (R - R_{\text{given}})^2$$

$$f_2 = [\cos \theta_0 - (\cos \theta_0)_{\text{given}}]^2 + [\sin \theta_0 - (\sin \theta_0)_{\text{given}}]^2 \quad (\text{B-1})$$

where the subscript "given" indicates the values of  $R$  and  $\theta_0$ ;  $R, \cos \theta_0$ , and  $\sin \theta_0$  are the values calculated from the selected set of  $(\Delta\phi, \Delta\psi)$ , and  $\phi^*, \psi^*$ , by means of eq 13-15. Then,  $\Delta\phi$  and  $\Delta\psi$  are varied to minimize to zero the values of the function

$$f = w_1 f_1 + w_2 f_2 \quad (\text{B-2})$$

where  $w_1$  and  $w_2$  are weighting factors that are chosen so that both terms on the right-hand side of eq B-2 change equally in the minimization process.

This process was repeated at each grid point  $(R, \theta_0)$ , in section III, to give a unique set of values of  $\Delta\phi, \Delta\psi$ , although it sometimes happened that no solution for  $\Delta\phi, \Delta\psi$  existed in the given range of  $\Delta\phi, \Delta\psi$  (i.e.,  $-20$  to  $20^\circ$ ).

#### References and Notes

- (1) This work was supported by research grants from the National Institute of General Medical Sciences, U.S. Public Health Service (GM-14312), and the National Science Foundation (BMS75-08691).
- (2) G. N. Ramachandran, *Treatise Collagen*, 1, 103 (1967).
- (3) A. Rich and F. H. C. Crick, *J. Mol. Biol.*, **3**, 483 (1961).
- (4) F. H. C. Crick, *Acta Crystallogr.*, **6**, 689 (1953).
- (5) R. D. B. Fraser and T. P. MacRae, *J. Mol. Biol.*, **3**, 640 (1961).
- (6) C. Cohen and K. C. Holmes, *J. Mol. Biol.*, **6**, 423 (1963).
- (7) D. A. D. Parry and J. M. Squire, *J. Mol. Biol.*, **75**, 33 (1973).
- (8) K. Okuyama, N. Tanaka, T. Ashida, and M. Kakudo, to be published.
- (9) F. H. C. Crick, *Acta Crystallogr.*, **6**, 685 (1953).
- (10) R. D. B. Fraser, T. P. MacRae, and A. Miller, *Acta Crystallogr.*, **17**, 813 (1964).
- (11) M. H. Miller and H. A. Scheraga, *J. Polym. Sci., Polym. Symp.*, in press.
- (12) A. J. Hopfinger and A. G. Walton, *J. Macromol. Sci., Phys.*, **3**(1), 171 (1969).
- (13) V. G. Tumanyan, *Biopolymers*, **9**, 955 (1970).
- (14) H. Sugeta and T. Miyazawa, *Biopolymers*, **5**, 673 (1967).
- (15) C. Chothia, *J. Mol. Biol.*, **75**, 295 (1973).
- (16) W. Traub and K. A. Piez, *Adv. Protein Chem.*, **25**, 243 (1971).
- (17) IUPAC-IUB Commission on Biochemical Nomenclature, *Biochemistry*, **9**, 3471 (1970).
- (18) D. A. D. Parry and E. Suzuki, *Biopolymers*, **7**, 199 (1969).
- (19) F. A. Momany, R. F. McGuire, A. W. Burgess, and H. A. Scheraga, *J. Phys. Chem.*, **79**, 2361 (1975).
- (20) S. Arnott, S. D. Dover, and A. Elliott, *J. Mol. Biol.*, **30**, 201 (1967).
- (21) A. Elliott, "Poly- $\alpha$ -Amino Acids", G. D. Fasman, Ed., Marcel Dekker, New York, N.Y., 1967, p 1.
- (22) R. F. McGuire, G. Vanderkooi, F. A. Momany, R. T. Ingwall, G. M. Crippen, N. Lotan, R. W. Tuttle, K. L. Kashuba, and H. A. Scheraga, *Macromolecules*, **4**, 112 (1971).
- (23) F. Colonna-Cesari, S. Premilat, and B. Lotz, *J. Mol. Biol.*, **95**, 71 (1975).
- (24) P. N. Lewis, F. A. Momany, and H. A. Scheraga, *Isr. J. Chem.*, **11**, 121 (1973).
- (25) Y. C. Fu, R. F. McGuire, and H. A. Scheraga, *Macromolecules*, **7**, 468 (1974).
- (26) L. Pauling and R. B. Corey, *Proc. Natl. Acad. Sci. U.S.A.*, **37**, 729 (1951).
- (27) R. D. B. Fraser, T. P. MacRae, D. A. D. Parry, and E. Suzuki, *Polymer*, **12**, 35 (1971).
- (28) L. Pauling and R. B. Corey, *Nature (London)*, **171**, 59 (1953).
- (29) R. D. B. Fraser and T. P. MacRae, "Conformation in Fibrous Proteins", Academic Press, New York, N.Y., 1973, p 421 (Figure 15.7a).
- (30) G. N. Ramachandran, V. Sasisekharan, and Y. T. Thathachari, "Collagen", N. Ramanathan, Ed., Wiley, New York, N.Y., 1962, p 81.
- (31) A. Yonath and W. Traub, *J. Mol. Biol.*, **43**, 461 (1969).